N71-36103

NASA CONTRACTOR REPORT

CASE FILE COPY

NASA CR-61358

HAZARD ESTIMATES FOR SELECTED ROCKET FUEL COMPONENTS AT KENNEDY SPACE CENTER

By R. K. Dumbauld and J. R. Bjorklund

GCA Technology Division
GCA Corporation
Bedford Park, Massachusetts

May 5, 1971

Prepared for

NASA-GEORGE C. MARSHALL SPACE FLIGHT CENTER
Marshall Space Flight Center, Alabama 35812

TECHNICAL REPORT STANDARD TITLE PAGE

1. REPORT NO. NASA CR-61358	2. GOVERNMENT ACCESSION NO.	3. RECIPIENT'S CATALOG NO.
4. TITLE AND SUBTITLE HAZARD ESTIMATES FOR SELECTED ROCKET FUEL COMPONENTS AT KENNEDY SPACE CENTER		5. REPORT DATE May 5, 1971
		6. PERFORMING ORGANIZATION CODE
7. AUTHOR (S) R. K. Dumbauld and J. R. Bjorklund		8. PERFORMING ORGANIZATION REPORT #
9. PERFORMING ORGANIZATION NAME AND ADDRESS GCA Technology Division GCA Corporation Bedford Park, Massachusetts		10. WORK UNIT NO.
		11. CONTRACT OR GRANT NO. NAS8-26673
		13. TYPE OF REPORT & PERIOD COVERED CONTRACTOR REPORT
12. SPONSORING AGENCY NAME AND ADDRESS National Aeronautics and Space Administration Washington, D. C. 20546		
		14. SPONSORING AGENCY CODE

15. SUPPLEMENTARY NOTES The NASA Contract Monitor was Mr. John W. Kaufman, Aerospace Environment Division, Aero-Astrodynamics Laboratory, Marshall Space Flight Center.

16. ABSTRACT

The results of this study represent estimates of hazard distances downwind for selected rocket fuel components from normal launches of Saturn V aerospace vehicles at Cape Kennedy. Listings of the fuel components studied, the maximum allowable concentrations for a ten-minute period considered in estimating the hazard distances, and the molecular weight of the components are provided. Calculations of concentrations for the three different meteorological situations used indicated that downwind hazard distances for normal launches of Saturn V vehicles were primarily dependent on the depth of the surface mixing layer and the vertical distribution of material in the stabilized cloud of exhaust products. A few exceptions were found, particularly with respect to the sea breeze which had a mixing depth of about 300 meters.

The concentration models applied in this analysis are by R. K. Dumbauld et al., and the estimates of maximum cloud rise were obtained from an expression due to B. A. Griggs. Normalized ground-level peak and ten-minute average concentrations for the fall, spring, and sea-breeze meteorological regimes are presented.

17. KEY WORDS surface mixing ground-level peak concentrations	18. DISTRIBUTION STATEMENT Unclassified-Unlimited E. D. GEISSLER, Director, Aero-Astrodynamics Laboratory, MSFC

19. SECURITY CLASSIF. (of this report)	20. SECURITY CLASSIF. (of this page)	21. NO. OF PAGES	22. PRICE
Unclassified	Unclassified	66	$3.00

MSFC - Form 3292 (May 1969)

TABLE OF CONTENTS

LIST OF TABLES

LIST OF FIGURES

LIST OF FIGURES (Continued)

LIST OF FIGURES (Continued)

LIST OF FIGURES (Continued)

SECTION 1
INTRODUCTION

Estimates have been made of hazard distances downwind from normal launches of Saturn V type aerospace vehicles at Cape Kennedy for selected rocket fuel components under three meteorological situations. The selected fuel components, the maximum allowable concentrations for a ten-minute exposure period (MAC_{10}) considered in estimating the hazard distances and the molecular weights of the components are given in Table 1-1.

The three meteorological situations used for the hazard calculations are based on the mean monthly wind speed, wind direction, and temperature profiles for Kennedy Space Center (KSC) published by Smith and Vaughan (1961) and on the work of Record, et al. (1970). Preliminary concentration calculations showed that downwind hazard distances for normal launches of Saturn V type vehicles were primarily dependent on the depth of the surface mixing layer H_m and the vertical distribution of material in the stabilized cloud of exhaust products. Study of the mean wind speed, wind direction, and temperature profiles for KSC showed that, for easterly wind flow required to transport the combustion product cloud inland, the average surface mixing depth was about 1000 meters. Two exceptions were noted. During the spring, there are a few occasions when the surface mixing depth is about 2000 meters; also, during the afternoon sea breeze in all seasons, the average surface mixing depth is about 300 meters. Figures 1-1, 1-2, and 1-3 show composite vertical profiles of air temperature, wind direction, and wind speed for easterly wind regimes in the fall and spring and for the afternoon sea breeze.

TABLE 1-1

MOLECULAR WEIGHTS AND 10-MINUTE MAXIMUM ALLOWABLE CONCENTRATIONS (MAC_{10}) FOR SELECTED ROCKET FUEL COMPONENTS

Fuel Component	Molecular Weight	MAC_{10}* (ppm)
CO	28.01	1500
HCl	36.47	30
NO_2	46.01	30
N_2O_4	92.02	30
N_2H_4	32.05	30
MMH	46.07	90
UDMH	60.00	100
F_2	38.00	15
HF	20.01	20
Al_2O_3	101.94	50 (mg m^{-3})

*Supplied by personnel of Atmospheric Dynamics Branch, Aerospace Environment Division, Aero-Astrodynamics Laboratory, George C. Marshall Space Flight Center, Marshall Space Flight Center, Alabama

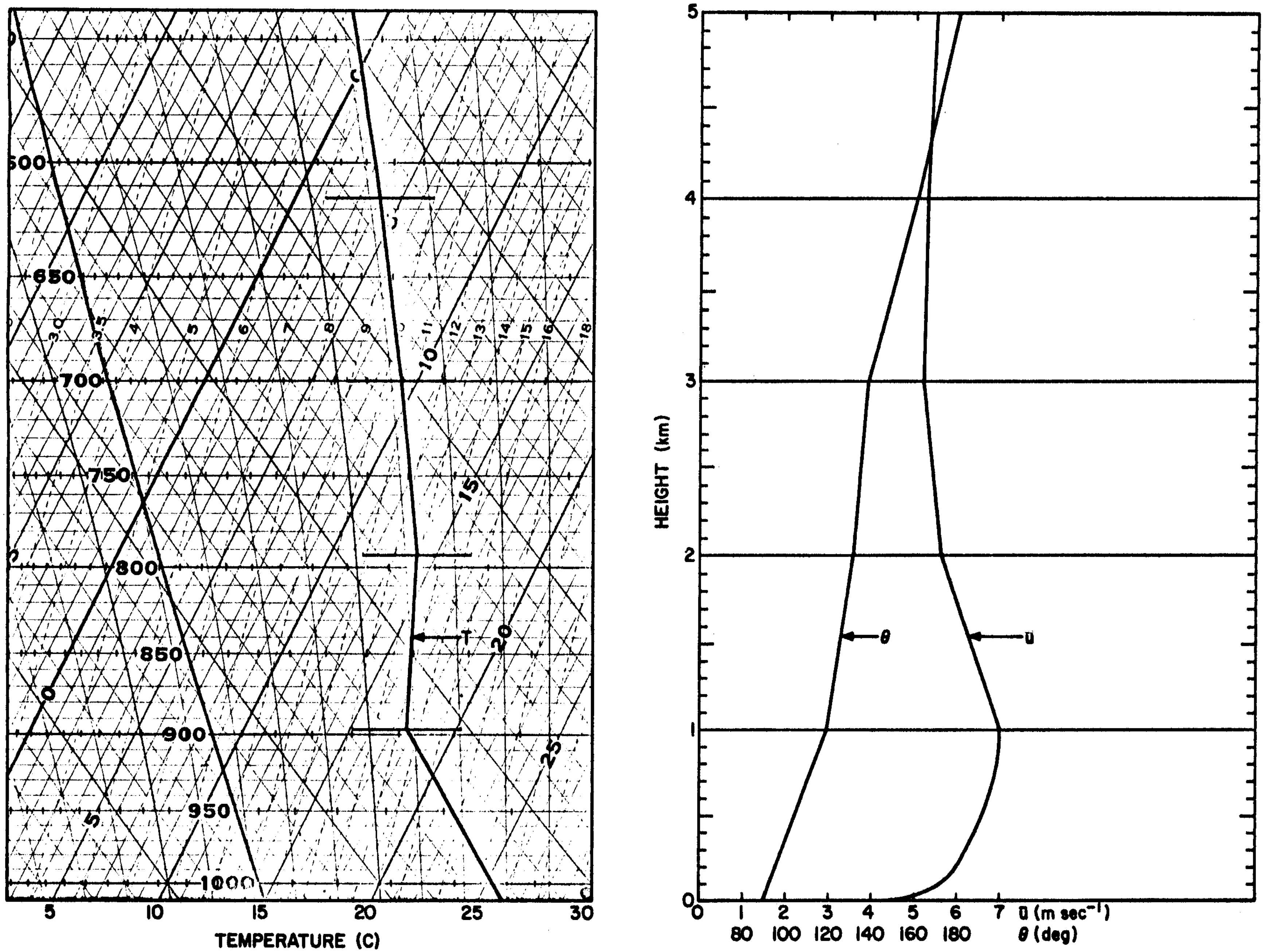

FIGURE 1-1. Vertical profiles of air temperature T, mean wind direction θ, and mean wind speed $\bar{u}$ for the fall meteorological regime at KSC. Heavy horizontal lines indicate layer boundaries.

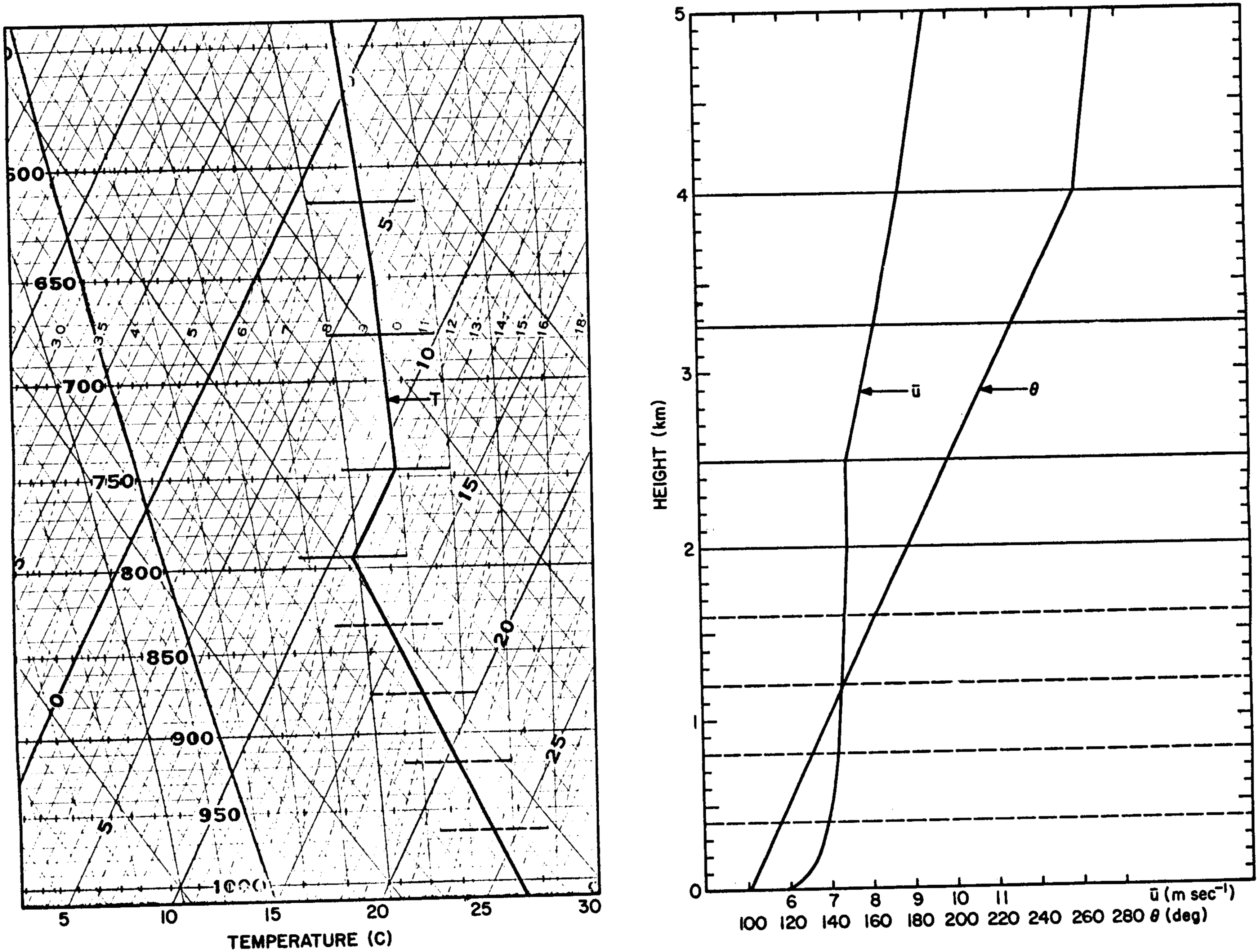

FIGURE 1-2. Vertical profiles of air temperature T, mean wind speed ū, and wind direction θ for the spring meteorological regime at KSC. Heavy solid and dashed horizontal lines indicate layer boundaries.

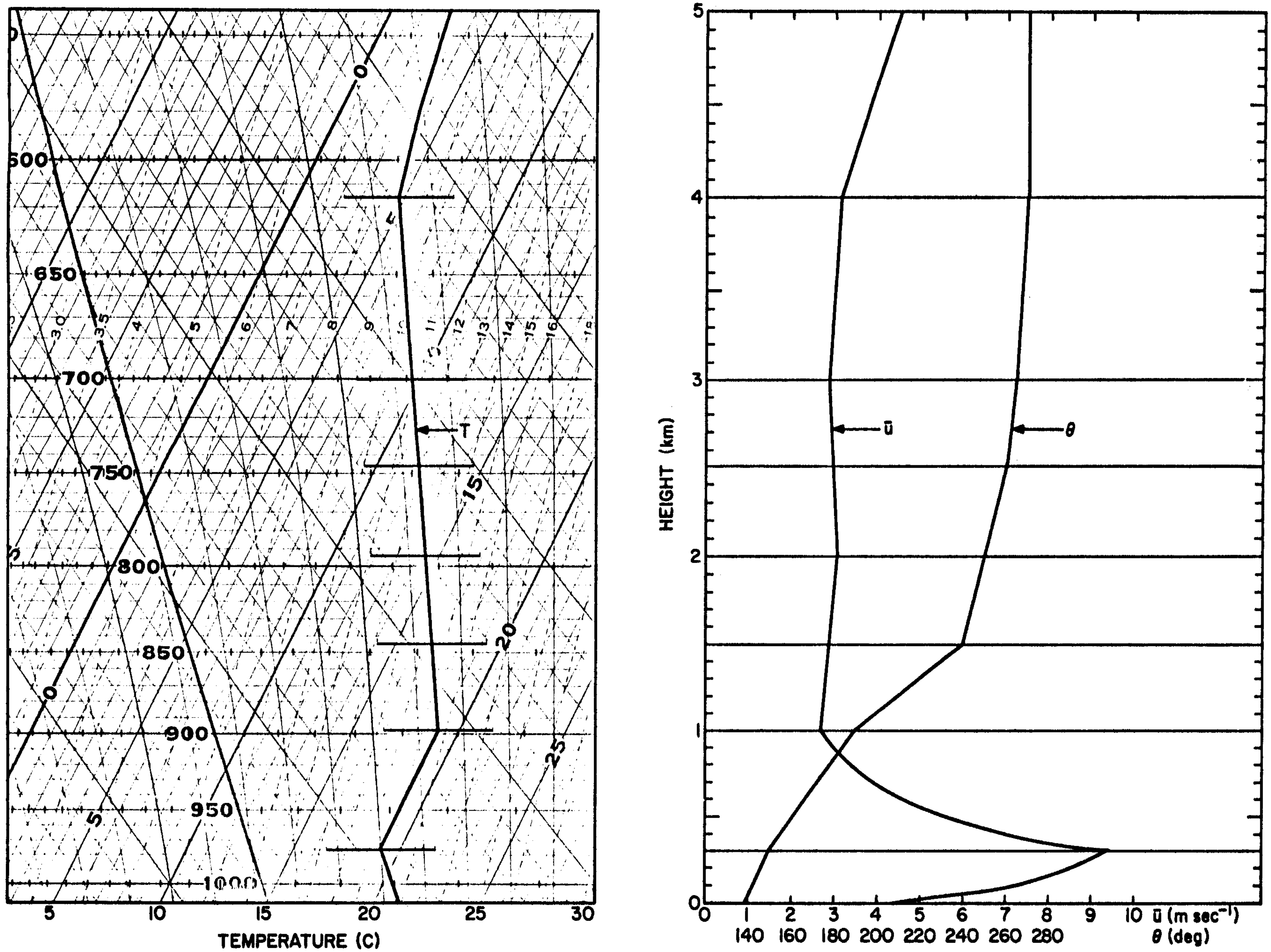

FIGURE 1-3. Vertical profiles of air temperature T, mean wind speed ū, and wind direction θ for the afternoon sea-breeze regime at KSC. Heavy horizontal lines indicate layer boundaries.

SECTION 2

CLOUD RISE CALCULATIONS

Estimates of maximum cloud rise for use in the hazard calculations were obtained from an expression due to Briggs (1969, p. 33; 1970):

$$z = \left[\frac{3F_m}{\bar{u}\,\gamma^2\, s^{1/2}} \sin\left(s^{1/2}\, t\right) + \frac{3F}{\bar{u}\,\gamma^2\, s} \left(1 - \cos\left(s^{1/2}\, t\right)\right)\right]^{1/3} \tag{2-1}$$

where

z = height of cloud at time t

$F_m = w_o^2\, r_o^2$

w_o = initial vertical velocity (m sec^{-1})

r_o = radius of area where vertical velocity equals w_o (m)

$\bar{u}$ = mean wind speed (m sec^{-1})

γ = entrainment constant where cloud radius $r\{z\} = \gamma z$

s = stability parameter $= \frac{g}{T} \frac{\partial \Phi}{\partial z}$

g = gravitational acceleration = 9.8 m sec^{-2}

T = ambient air temperature (^oK)

$\frac{\partial \Phi}{\partial z}$ = vertical potential temperature gradient ($^oK\ m^{-1}$)

$F = \frac{g\, Q_H}{\pi\, c_p\, \rho\, T}$

Q_H = heat emission due to efflux of hot gases (cal sec^{-1})

c_p = specific heat of air = 0.24 cal $g^{-1}\ {}^oK^{-1}$

ρ = density of air (g m^{-3})

t = time (sec)

The above formula yields cloud rise rates that agree favorably with measured cloud rise rates from static tests of Saturn type engines published by Susko, Kaufman, and Hill (1968).

Input parameters used in the calculation of maximum cloud rise are shown in Table 2-1. The value of Q_H in the table was calculated from the expression

$$Q_H = c_{pm} T_m W$$

where

c_{pm} = specific heat of exhaust gas = 0.49 cal g^{-1} $^{o}K^{-1}$

T_m = temperature of exhaust gas = 2080^{o}K

W = mass of exhaust gas burned per unit time = 2.268×10^{6} g sec^{-1} $engine^{-1}$

Thus, for the five F-1 engines as employed on the first stage of Saturn V, the value for Q_H equals 1.155×10^{10} cal sec^{-1}. The values of c_{pm}, T_m, W, and w_o were obtained from a report by Thayer, Chandler and Chu (1970). A value of 0.5 for the entrainment constant γ was chosen because Dumbauld (1971) found that this value provided the best fit of Equation (2-1) to the rate of cloud rise data from static engine tests mentioned above. Values for the meteorological parameters in Table 2-1 were obtained from Figures 1-1, 1-2, and 1-3.

The maximum cloud rise calculated from Equation (2-1) for the fall, spring, and sea-breeze meteorological regimes is, respectively, 2270, 2200, and 2260 meters.

It should be mentioned that, although the rate of cloud rise is highly dependent on the value of parameters in the first term of Equation (2-1), the

TABLE 2-1

INPUT PARAMETERS TO PLUME RISE FORMULA

(a) General	
w_o^* = 488 m sec^{-1}	Q_H^* = 1.155×10^{10} cal sec^{-1}
r_o = 5 m	γ = 0.5
ρ = 1190 g m^{-3}	c_p = 0.24 cal g^{-1} $^oK^{-1}$

(b) Specific	Meteorological Regime		
	Fall	Spring	Sea Breeze
T (^oK)	299	300	294
$\partial\Phi/\partial z$ (^oK m^{-1})	0.0044	0.0040	0.0064
$\bar{u}$ (m sec^{-1})	6.0	7.2	4.2

*From report by Thayer, Chandler, and Chu (1970).

maximum cloud rise depends more on the values assigned to the parameters in the second term. The maximum cloud rise z_m can thus be estimated with sufficient accuracy from the expression

$$z_m = \left[\frac{6F}{\bar{u}\,\gamma^2\, s}\right]^{1/3} \tag{2-2}$$

SECTION 3

VERTICAL DISTRIBUTION OF ROCKET COMBUSTION PRODUCTS AND INITIAL CLOUD DIMENSIONS

The material in the cloud of combustion products from a normal launch is composed of two parts:

- The contribution from the first 30 seconds' operation of the rocket motors which is assumed to be entirely contained in the stabilized ground cloud

- The contribution from the operation of the rocket motors as the vehicle ascends from a height of 1236 meters (the height after 30 seconds) to 5 kilometers (the height after 56 seconds)

The geometry of the stabilized cloud of combustion products for the fall, spring, and sea-breeze meteorological regimes is shown in Figures 3-1, 3-2, and 3-3. The slanted solid lines between ground level and the height of maximum cloud rise show the diameter of the stabilized ground cloud calculated from the expression

$$r\{z\} = \gamma\left(z - z_o + r_o/\gamma\right) \; ; \; 0 \le z \le z_m \tag{3-1}$$

where

r_o = initial radius of the cloud at height z_o

z_m = height of maximum cloud rise

The entrainment parameter, as before, is set equal to 0.5. The initial radius r_o and height z_o were set equal to 454.3 meters. These values of r_o and z_o are consistent with cloud dimensions determined 30 seconds after ignition from time

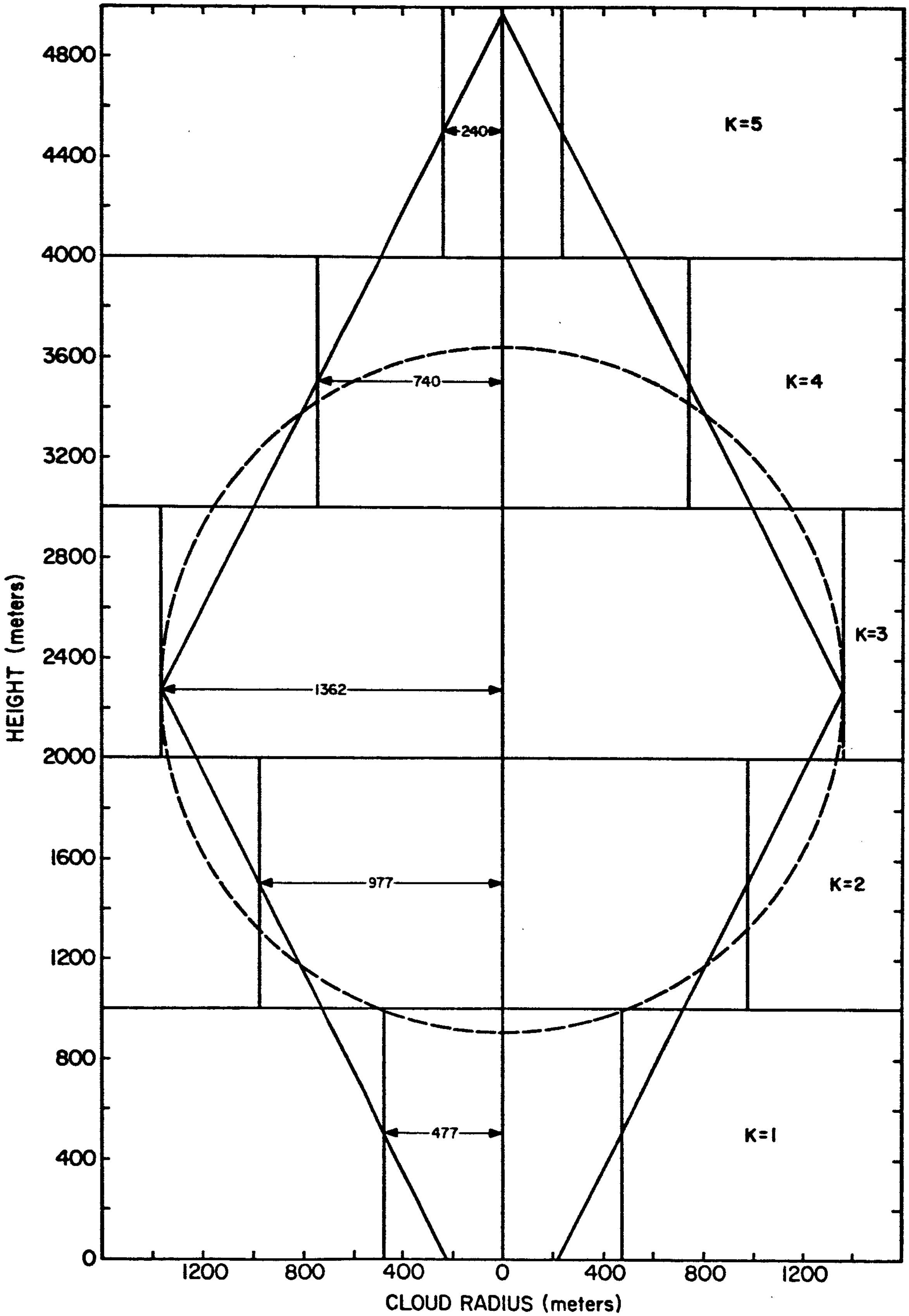

FIGURE 3-1. Geometry of the cloud of combustion products between ground level and 5 kilometers for the fall meteorological regime.

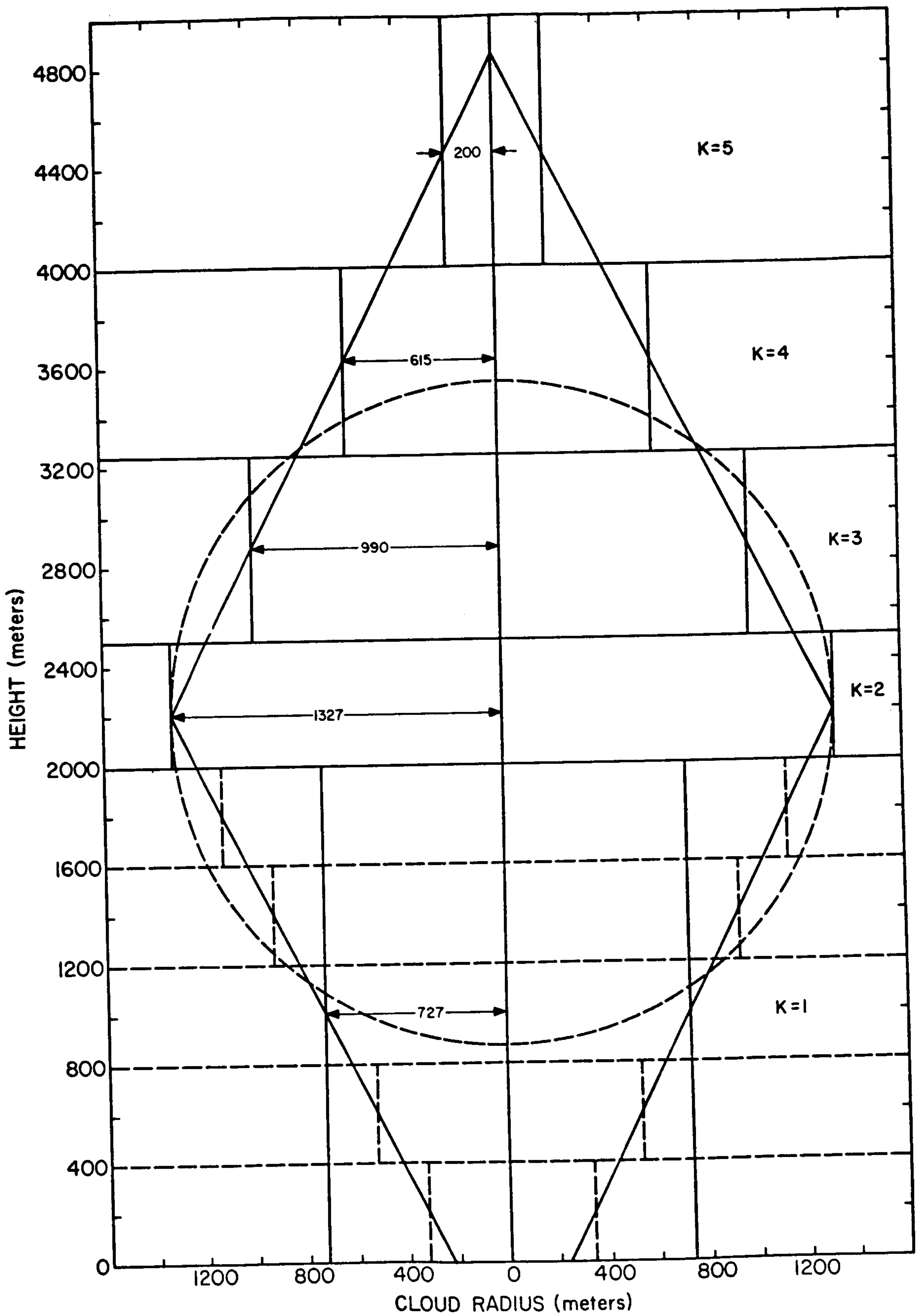

FIGURE 3-2. Geometry of the cloud of combustion products between ground level and 5 kilometers for the spring meteorological regime.

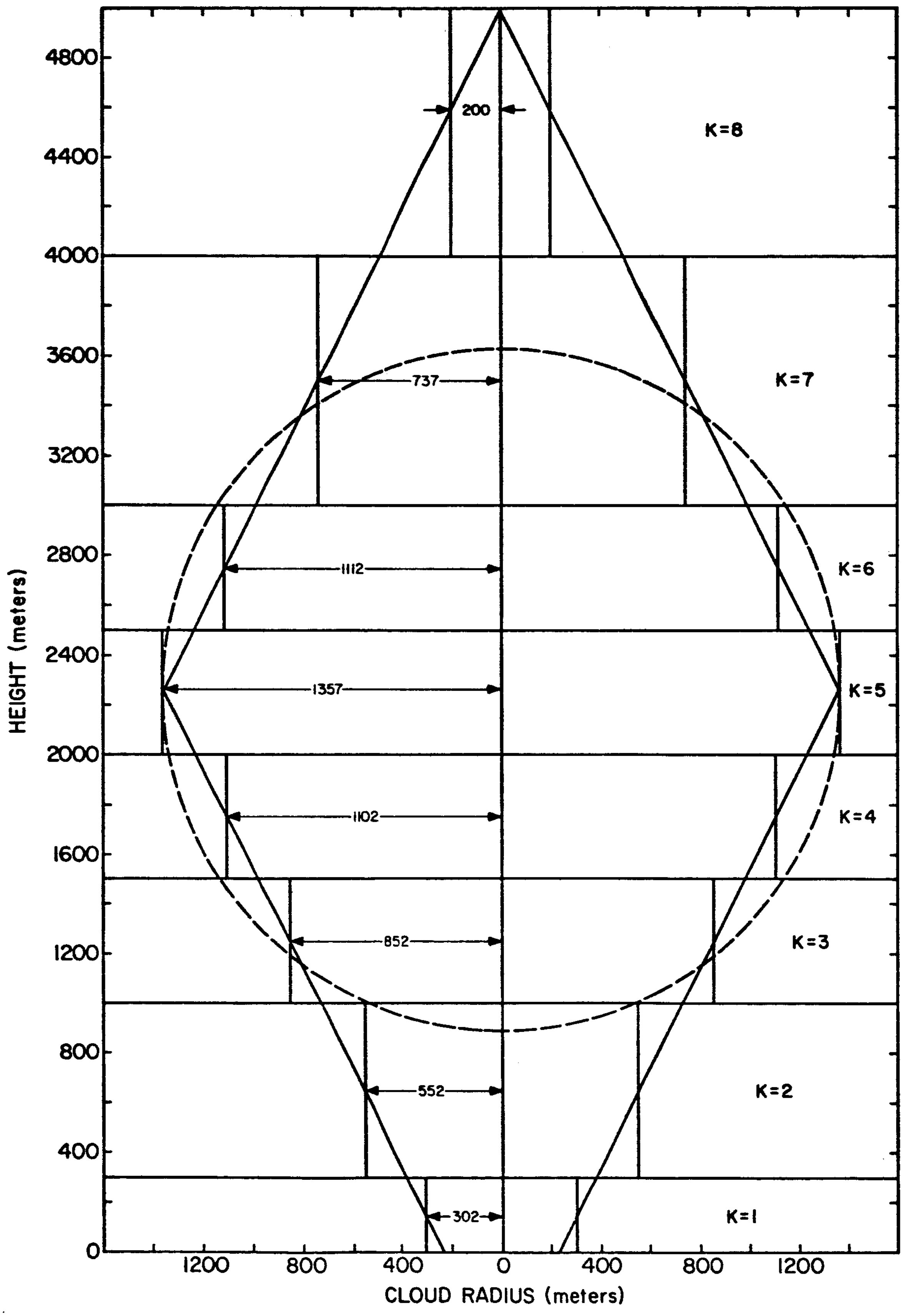

FIGURE 3-3. Geometry of the cloud of combustion products between ground level and 5 kilometers for the sea-breeze meteorological regime.

sequence photographs of the launch of Apollo 10. The slanted solid lines defining the cloud diameter above z_m are constructed from the expression

$$r\{z\} = z_m - \gamma\left(z + z_o - \frac{r_o}{\gamma}\right) \geq 200; \; z \geq z_m \tag{3-2}$$

and are mirror images of the lines defining the cloud diameters below z_m. It should be noted that $r\{z\}$ in this case is not permitted to become less than 200 meters.

The solid horizontal lines in Figures 3-1, 3-2, and 3-3 show the layer structure of the atmosphere based on the variations of meteorological profile quantities described in Section 1. The dashed horizontal lines shown in Figure 3-2 for the spring meteorological regime indicate an alternate division of the layer structure used to estimate ground-level concentrations.

The dashed circle in Figures 3-1, 3-2, and 3-3 shows the 2.15 σ limits for a Gaussian distribution centered at z_m, where the standard deviation σ of the distribution is defined by

$$\sigma = \frac{r\{z = z_m\}}{2.15} \tag{3-3}$$

The fraction of material F_g in each layer from the initial 30 seconds' operation of the rocket motors is given by the expression

$$F_g = \left\{ P\{z_{TK}\} \left[\frac{z_{TK} - z_{max}}{\sigma}\right] - P\{z_{BK}\} \left[\frac{z_{BK} - z_{max}}{\sigma}\right] \right\} \tag{3-4}$$

where

F_g = fraction of material from initial 30 seconds' emission found in the layer

$P\{z_{TK}\}$ = integral of the Gaussian (normal) probability function between minus infinity and the top of the K^{th} layer z_{TK}

$P\{z_{BK}\}$ = integral of the Gaussian (normal) probability function between minus infinity and the bottom of the K^{th} layer z_{BK}

Material is also added in the lowest 5 kilometers of the atmosphere by vehicle emission subsequent to the initial 30 seconds. Figure E-7 of the NASA report by Dumbauld, et al. (1970) describes the altitude of the Saturn vehicle as a function of time after ignition. The time required for the Saturn vehicle to reach a given altitude $\leq$ 5 kilometers (t $\leq$ 56 seconds) is given by the expression

$$t_v = 1.25\,(z)^{0.44636} \quad ; \quad z \leq 5000\text{ m} \tag{3-5}$$

where

t_v = time after ignition (sec)

z = Saturn altitude (m)

The total fraction F_T of material in any layer resulting from Saturn emissions over the first 56 seconds of flight, during which the vehicle reaches an altitude of 5 kilometers, is given by the expressions

$$F_{TK} = \left\{ \begin{array}{ll} \frac{30}{56}\,F & ;\; z_{TK} \leq 1{,}236\text{ m} \\ \frac{30}{56}\,F + \left(\frac{1.25\, z_{TK}^{\;0.44636} - 30}{56} \right) & ;\; z_{TK} > 1{,}236\text{m},\; z_{BK} < 1{,}236\text{m} \\ \frac{30}{56}\,F + \frac{1.25}{56}\left(z_{TK}^{\;0.44636} - z_{BK}^{\;0.44636} \right) & ;\; z_{TK} > 1{,}236\text{m},\; z_{BK} > 1{,}236\text{m} \end{array} \right\} \tag{3-6}$$

Table 3-1 gives values of F_{TK} calculated from Equation (3-6) for the three meteorological regimes. The two columns under the spring meteorological regime represent the distribution of material based on the meteorological layer structure (1) and the additional layer structure for better definition of ground-level concentration (2).

The initial lateral $\left(\sigma_{yo}\{K\}\right)$ and alongwind $\left(\sigma_{xo}\{K\}\right)$ cloud dimensions for the K^{th} layer are determined from the average radius of the ground cloud in the layer. The average cloud diameters are shown in Figures 3-1, 3-2, and 3-3 as solid vertical lines and the corresponding cloud radii are given by the numerical values printed in the figures. The expressions used to calculate the cloud dimensions are

$$\sigma_{yo}\{K\} = \sigma_{xo}\{K\} = \left\{H - \gamma\left[\left(\frac{z_{TK} + z_{BK}}{2}\right) - \frac{r_o}{\gamma} + z_o\right]\right\}\bigg/ 2.15 \qquad (3\text{-}7)$$

when the K^{th} layer is above the layer containing z_m;

$$\sigma_{yo}\{K\} = \sigma_{xo}\{K\} = \left\{\gamma\left[z_m + \frac{r_o}{\gamma} - z_o\right]\right\}\bigg/ 2.15 \qquad (3\text{-}8)$$

when the K^{th} layer contains z_m; and

$$\sigma_{yo}\{K\} = \sigma_{xo}\{K\} = \left\{\gamma\left[\left(\frac{z_{TK} - z_{BK}}{2}\right) + \frac{r_o}{\gamma} - z_o\right]\right\}\bigg/ 2.15 \qquad (3\text{-}9)$$

when the K^{th} layer is below the layer containing z_m. The minimum initial cloud dimensions permitted in any layer are

$$\sigma_{yo}\{K\} = \sigma_{xo}\{K\} = \frac{200}{2.15} = 93 \text{ meters} \qquad (3\text{-}10)$$

The initial cloud dimensions calculated for the three meteorological regimes calculated from Equations (3-7) through (3-10) are given in Table 3-2.

TABLE 3-1

TOTAL FRACTION OF MATERIAL (F_{TK}) IN THE K^{th} LAYER FROM SATURN EXHAUST EMISSIONS*

Layer (K)	Meteorological Regime			
	Fall	Spring		Sea Breeze
		(1)	(2)	
1	0.012	0.328	0.0009	0.0005
2	0.296	0.238	0.005	0.012
3	0.421	0.235	0.022	0.097
4	0.174	0.103	0.126	0.201
5	0.096	0.096	0.174	0.234
6			0.238	0.186
7			0.235	0.172
8			0.103	0.097
9			0.096	

*Fractions may not add to unity because of round-off errors.

TABLE 3-2

INITIAL CLOUD DIMENSIONS IN THE Kth LAYER

$\left(\sigma_{xo}\{K\} = \sigma_{yo}\{K\} \text{ in meters}\right)$

Layer (K)	Meteorological Regime			
	Fall	Spring (1)	Spring (2)	Sea Breeze
1	222	338	152	140
2	454	617	245	257
3	632	461	338	396
4	344	286	431	513
5	112	93	524	631
6			617	517
7			461	343
8			286	93
9			93	

SECTION 4

CONCENTRATION MODELS

With exception of the dispersion model for calculating time-averaged concentrations, the models described in this section are documented in detail in a report prepared for NASA-Huntsville (Dumbauld, et al., 1970). A description of the time-averaged concentration model is included in a revised version of the above-mentioned report to be submitted to NASA in May 1971. For these reasons, only a brief description of the models is given in this section.

Peak concentrations in the K^{th} layer along the axis of cloud travel were calculated for the three meteorological regimes described above from the expression

$$\chi_p = \frac{Q_K}{2\pi \, \sigma_{yK} \, \sigma_{xK}} \tag{4-1}$$

where

Q_K = source strength in units of mass per unit depth of the K^{th} layer

σ_{yK} = standard deviation of the crosswind concentration distribution in the K^{th} layer

σ_{xK} = standard deviation of the alongwind concentration distribution in the K^{th} layer

Equation (4-1) above and the subset of equations defining σ_{yK} and σ_{xK} are given on pages 14 through 20 of the report by Dumbauld, et al. (1970). The use of Equation (4-1) implies that material originating in the K^{th} layer is constrained from diffusing vertically beyond the vertical boundaries of that layer.

Estimates were also made of ground-level peak concentration for the spring meteorological regime where the lowest 2 kilometers of the atmosphere is further subdivided into layers based on the vertical distribution of material (see columns labeled (2) in Tables 3-1 and 3-2). In this case, material contained in the layers below 2 kilometers indicated by horizontal dashed lines in Figure 3-2 must be permitted to diffuse vertically into the surface mixing layer because there is no meteorological restriction to mixing in the lowest 2 kilometers. The layer transition model described as Model 5 by Dumbauld, et al. (1970, pp. 31-33) proves to be a useful mathematical artifice for permitting the requisite vertical mixing while identifying the initial vertical structure of material. In the model, material in the original K layers is permitted to diffuse into a new layer (in this case the lowest 2 kilometers) at a predetermined time t*. For these calculations t* was set equal to 1 second. The hazard estimates using the layer transition model are compared to those obtained using Equation (4-1) for the spring meteorological regime in Section 6.

Time-average concentrations were calculated from the expression

$$\chi_{ave} = \frac{\chi_p \sqrt{2\pi}\, \sigma_{xK}}{\bar{u}_K T_A} \left\{ \operatorname{erf}\left(\frac{\bar{u}_K T_A}{2\sqrt{2}\, \sigma_{xK}} \right) \right\} \tag{4-2}$$

where

$\bar{u}_K$ = mean transport speed in the K^{th} layer

T_A = time over which concentration is averaged in seconds

SECTION 5
MODEL INPUTS

Initial cloud dimensions used in the hazard calculations are given in Table 3-2 and the vertical distributions of rocket exhaust products emitted during the first 56 seconds of a normal Saturn vehicle launch are given in Table 3-1. To simplify the computer calculations, the source strength in each layer was normalized. The results of the computer calculations must be multiplied by a simple scaling factor to obtain the concentration for a specific fuel component. Normalized source strengths shown in Table 5-1 were computed from the expression

$$Q_K = \frac{\left(F_{TK}\right)(T)\ 22.4 \times 10^3}{\left(z_{TK} - z_{BK}\right) 273.2} \quad . \tag{5-1}$$

where F_{TK} is the fractional percent in the K^{th} layer from Table 3-1, and $\left(z_{TK} - z_{BK}\right)$ is the depth of the layer. The value of temperature T in the layer was set equal to 294 degrees for the fall and sea-breeze meteorological regimes and to 299 degrees for the spring meteorological regime.

Additional meteorological inputs are given in Table 5-2. Values of the mean wind speed $\bar{u}_{BK}$ and wind direction θ_{BK} at the base of the K^{th} layer were determined from the vertical profiles shown in Figures 1-1 through 1-3. Values of the standard deviation of the wind azimuth angle at the reference height $z_R = 18$ meters, for a 10-minute sampling period $\left(\tau_{oK} = 600 \text{ seconds}\right)$, were obtained from the expression

$$\sigma_{ABK} \left\{ \tau_{oK} = 600 \text{ sec} \ ; K = 1 \right\} = \frac{R_d}{6} \tag{5-2}$$

where R_d is the wind direction range at the reference height z_R from Figure 2-11 of the report by Record, et al. (1970). The quantity σ_A was assumed to decrease

TABLE 5-1

NORMALIZED SOURCE STRENGTHS Q_K

Layer (K)	Meteorological Regime			
	Fall	Spring		Sea Breeze
		(1)	(2)	
1	0.2905	4.019	0.0582	0.0402
2	7.130	11.634	0.3245	0.4064
3	10.160	7.684	1.341	4.687
4	41.970	3.364	7.708	9.692
5	23.350	2.354	10.660	11.301
6			11.634	8.973
7			7.684	4.147
8			3.364	2.331
9			2.354	

TABLE 5-2

ADDITIONAL METEOROLOGICAL INPUTS TO THE HAZARD CALCULATIONS

Regime	Parameter	Layer (K)									
		1	2	3	4	5	6	7	8	9	10
Fall	$\bar{u}_{BK}$ (m sec^{-1})	4.7	7.0	5.6	5.2	5.3	5.5				
	θ_{BK} (deg)	90	119	131	138	161	180				
	$\sigma_{ABK}\{\tau_{oK}\}$ (deg)	12	8	1	1	1	1				
Spring	$\bar{u}_{BK}$ (m sec^{-1})	6	6.9	7.2	7.3	7.4	7.5	7.5	8.2	8.8	9.5
	θ_{BK} (deg)	100	116	133	148	164	180	200	230	260	270
	$\sigma_{ABK}\{\tau_{oK}\}$ (deg)	7	6.04	5.85	5.74	5.66	5.60	1	1	1	1
Sea Breeze	$\bar{u}_{BK}$ (m sec^{-1})	4.5	9.5	2.7	2.9	3.1	3.0	2.9	3.2	4.5	
	θ_{BK} (deg)	140	150	190	240	250	260	265	270	270	
	$\sigma_{ABK}\{\tau_{oK}\}$ (deg)	12	5.7	1	1	1	1	1	1	1	

with height according to the expression

$$\sigma_A\{z, K{=}1\} = \sigma_{ABK}\{z{=}z_R, K{=}1\} \left(\frac{z}{z_R}\right)^{-p} \tag{5-3}$$

as suggested by Record, et al. (1970, p. 48).

The power-law exponent p in Equation (5-3) is given by the expression

$$p = \log\left(\frac{\bar{u}_{TK}\{K{=}1\}}{\bar{u}_{BK}\{z_R, K{=}1\}}\right) \Bigg/ \log\left(\frac{z_{TK}\{K{=}1\}}{z_R}\right)$$

Note that a reference height of $z_R = 18$ meters was used for all meteorological parameters in the surface mixing layer. In the next higher layer ($K = 2$), the value of σ_A was linearly decreased from the value at the top of the surface layer to a value of 1.0 degrees at the top of the $K = 2$ layer. In all higher layers ($K > 2$), σ_A was held constant at 1.0 degrees.

SECTION 6

RESULTS OF THE HAZARD CALCULATIONS

Figures 6-1, 6-2, and 6-3 show normalized ground-level peak and ten-minute average concentrations for the fall, spring, and sea-breeze meteorological regimes obtained from Equations (4-1) and (4-2) above. In each case, the normalized source strengths given in Table 5-1 were used in the calculations. The layer structure for these calculations is shown by the solid horizontal lines in Figures 3-1, 3-2, and 3-3. The normalized concentrations are given in units of parts per million mole per gram of material released in the first 56 seconds after ignition. To obtain the concentration in parts per million (ppm) for the fuel components listed in Table 1-1, the concentrations in the figures must be multiplied by the total amount of material in grams released in the first 56 seconds following ignition and divided by the molecular weight of the material in grams. For example, suppose that 10^8 grams of hydrogen fluoride (HF) were actually released in the lowest 5 kilometers in the fall season. The ten-minute average concentration at 10,000 meters from the source is found from Figure 6-1 by entering the graph at 10^4 meters and obtaining a normalized concentration of 1.9×10^{-8} ppm mole g^{-1}; multiplying by the source strength in grams; and dividing by the molecular weight of HF (20.008). Thus,

$$\chi_{10\ \mathrm{min}}(\mathrm{HF}) = \frac{1.9 \times 10^{-8}\ (10^8)}{20.008} = 9.5 \times 10^{-2}\ \mathrm{ppm}$$

Figure 6-4 shows normalized ground-level peak and ten-minute average concentrations for the spring meteorological regime, calculated by means of the layer transition model discussed in Section 4 above and the layer structure in the lowest 2 kilometers as indicated by the dashed horizontal lines in Figure 3-2. In contrast to the normalized concentration shown in Figure 6-2 for the spring meteorological regime, the ground-level concentrations shown in Figure 6-4 are an order of

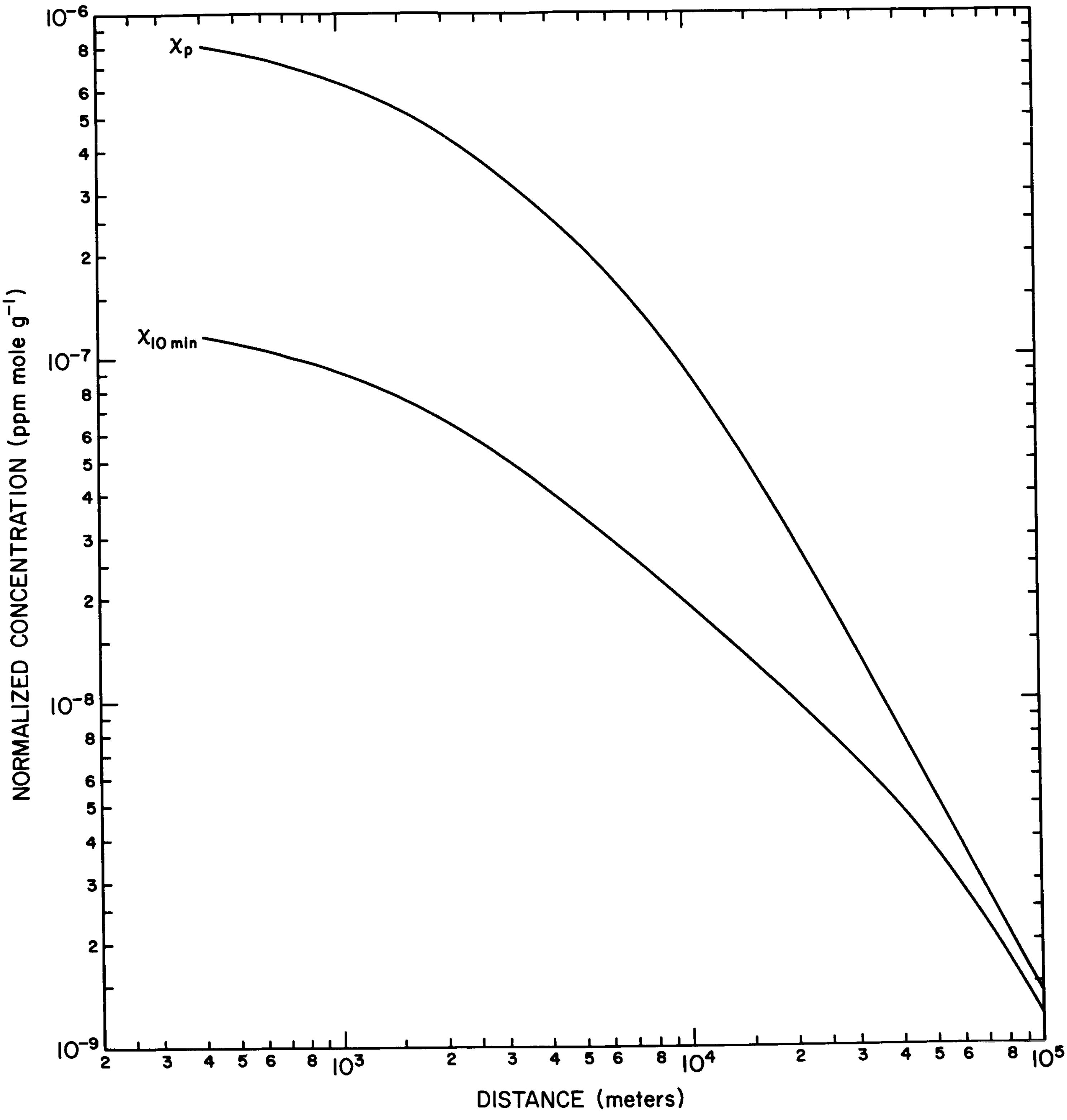

FIGURE 6-1. Normalized ground-level peak (χ_p) and ten-minute average ($\chi_{10\ min}$) concentrations downwind from a normal Saturn V launch for the fall-season meteorological regime. Source strength is one gram of material released in first 5 kilometers.

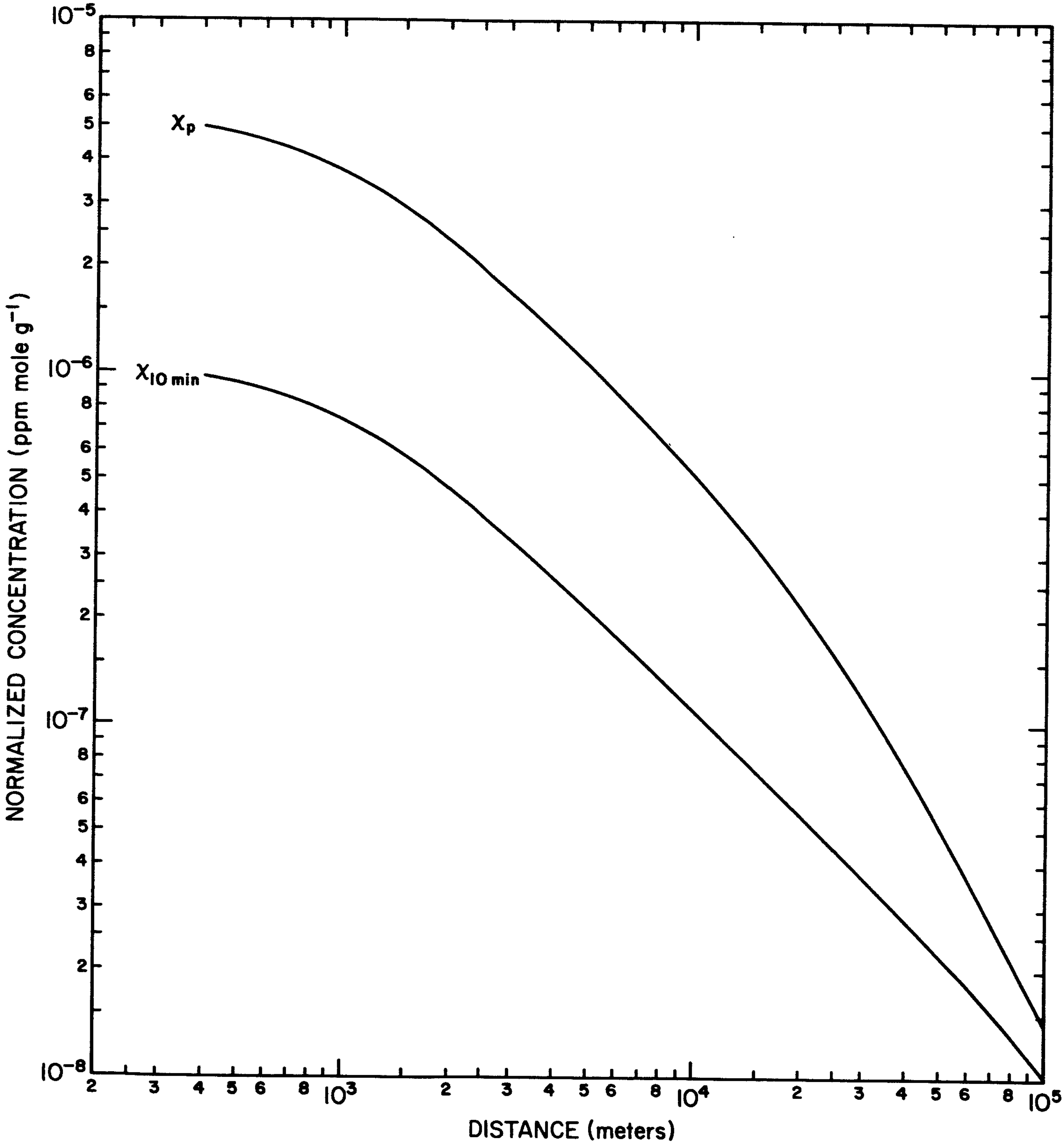

FIGURE 6-2. Normalized ground-level peak (χ_p) and ten-minute average ($\chi_{10\ min}$) concentrations downwind from a normal Saturn V launch for the spring meteorological regime. Source strength is one gram of material released in first 5 kilometers.

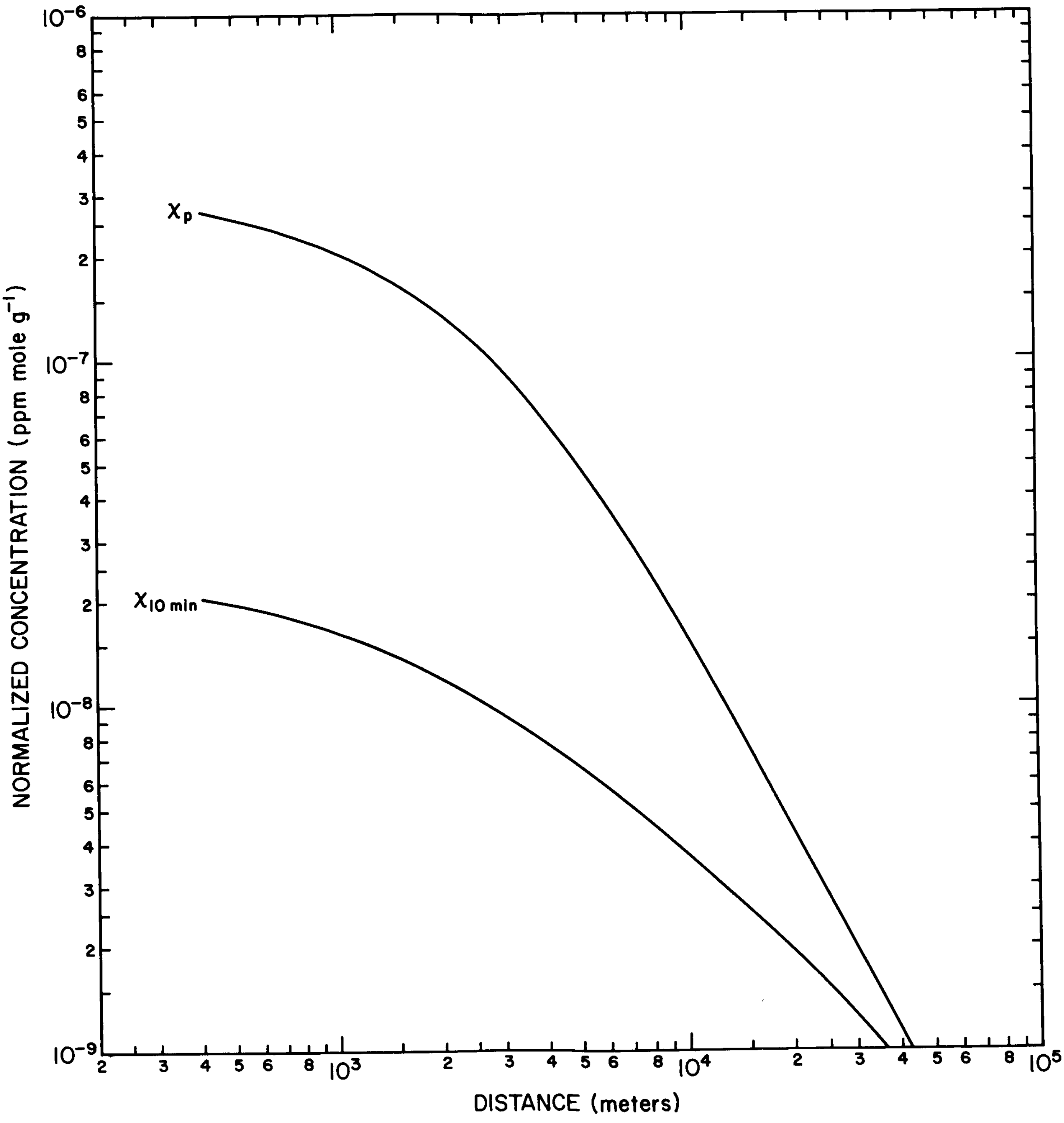

FIGURE 6-3. Normalized ground-level peak (χ_p) and ten-minute average ($\chi_{10\ min}$) concentrations downwind from a normal Saturn V launch for the sea-breeze meteorological regime. Source strength is one gram of material released in first 5 kilometers.

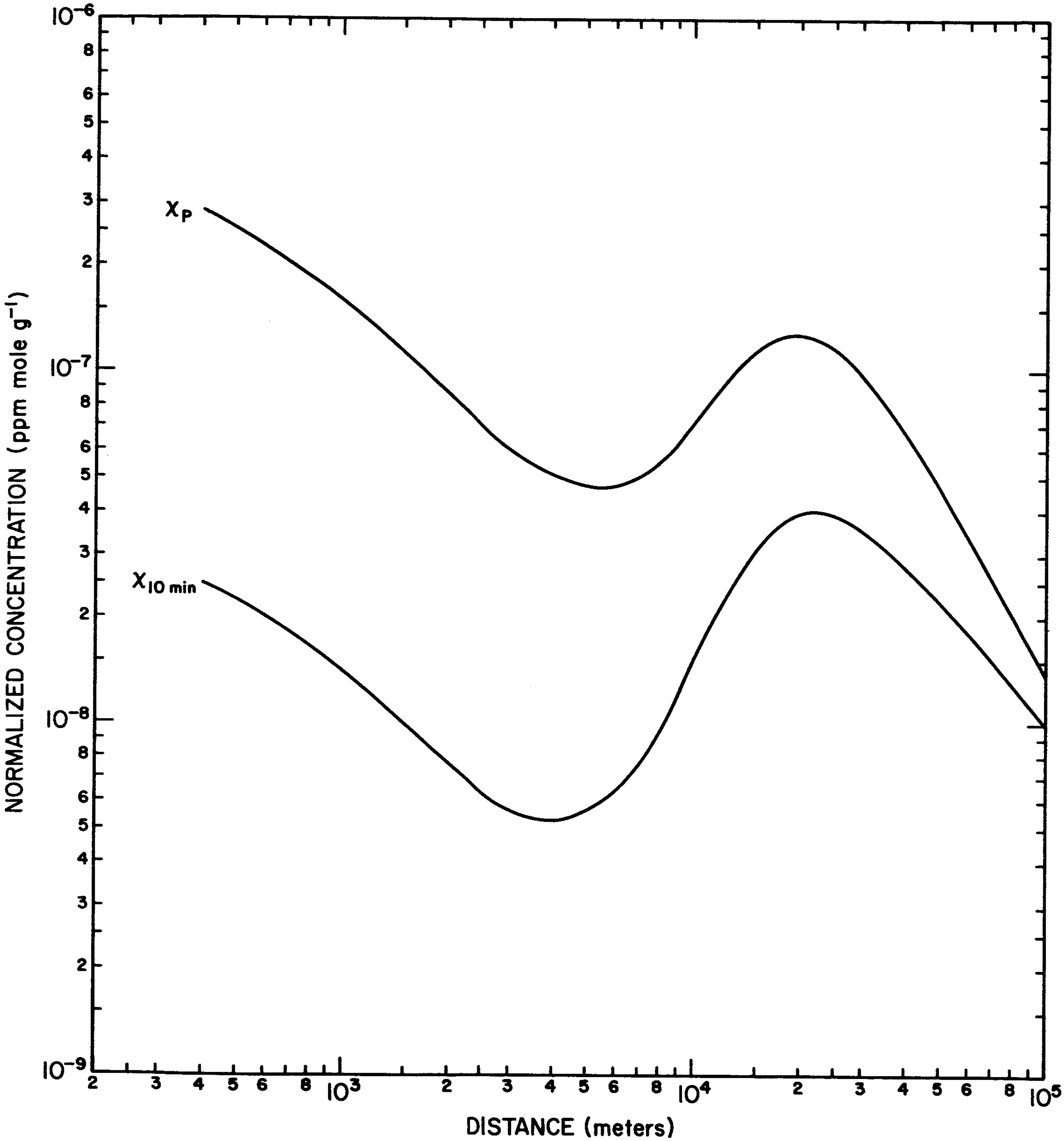

FIGURE 6-4. Normalized ground-level peak (χ_p) and ten-minute average ($\chi_{10\text{-}min}$) concentrations downwind from a normal Saturn V launch for the spring meteorological regime. Calculations were made using the layer transition model. Source strength is one gram of material released in first 5 kilometers.

magnitude lower in the first 4 kilometers downwind from the source. Beyond 4 kilometers, the concentrations shown in Figure 6-4 increase to a distance of about 25 kilometers from the source at which point they become nearly equivalent to the concentrations shown in Figure 6-2. The lower concentrations near the source predicted by the layer transition model are caused by the high initial concentration of material at the top of the surface mixing layer. In using the layer transition model, the material near the top of the layer is brought to the surface through turbulent mixing. As shown in Figure 6-4, complete vertical mixing has occurred in the layer transition case when the cloud reaches a downwind distance of 30 kilometers. In calculating the normalized ground-level concentrations shown in Figure 6-2, it has been assumed that the material is completely mixed in the surface layer (K = 1) prior to downwind travel from the source.

Although the concentration estimates shown in Figure 6-4 for the spring meteorological regime are likely more realistic than those shown in Figure 6-2, an arbitrary decision was made to use the estimates shown in Figure 6-2 in developing the remaining hazard estimates described in this section. This decision was made primarily because the use of the estimates from Figure 6-2 leads to more conservative hazard estimates.

Figures 6-5, 6-6, and 6-7 also show plots of ground-level peak concentration and 10-minute average concentrations for the three meteorological regimes These graphs are similar to those in Figures 6-1, 6-2, and 6-3, with the exception that the source strength used to normalize the figures is one pound of material released in the surface mixing layer. Concentrations in parts per million for specific materials can be obtained from the normalized values through multiplication by the source strength in the surface layer in pounds, and dividing by the appropriate molecular weight in grams. The surface mixing layer depths used in the calculations for the fall, spring, and sea-breeze regimes are: 1000, 2000, and 300 meters. Estimates of concentrations for other mixing layer depths can be

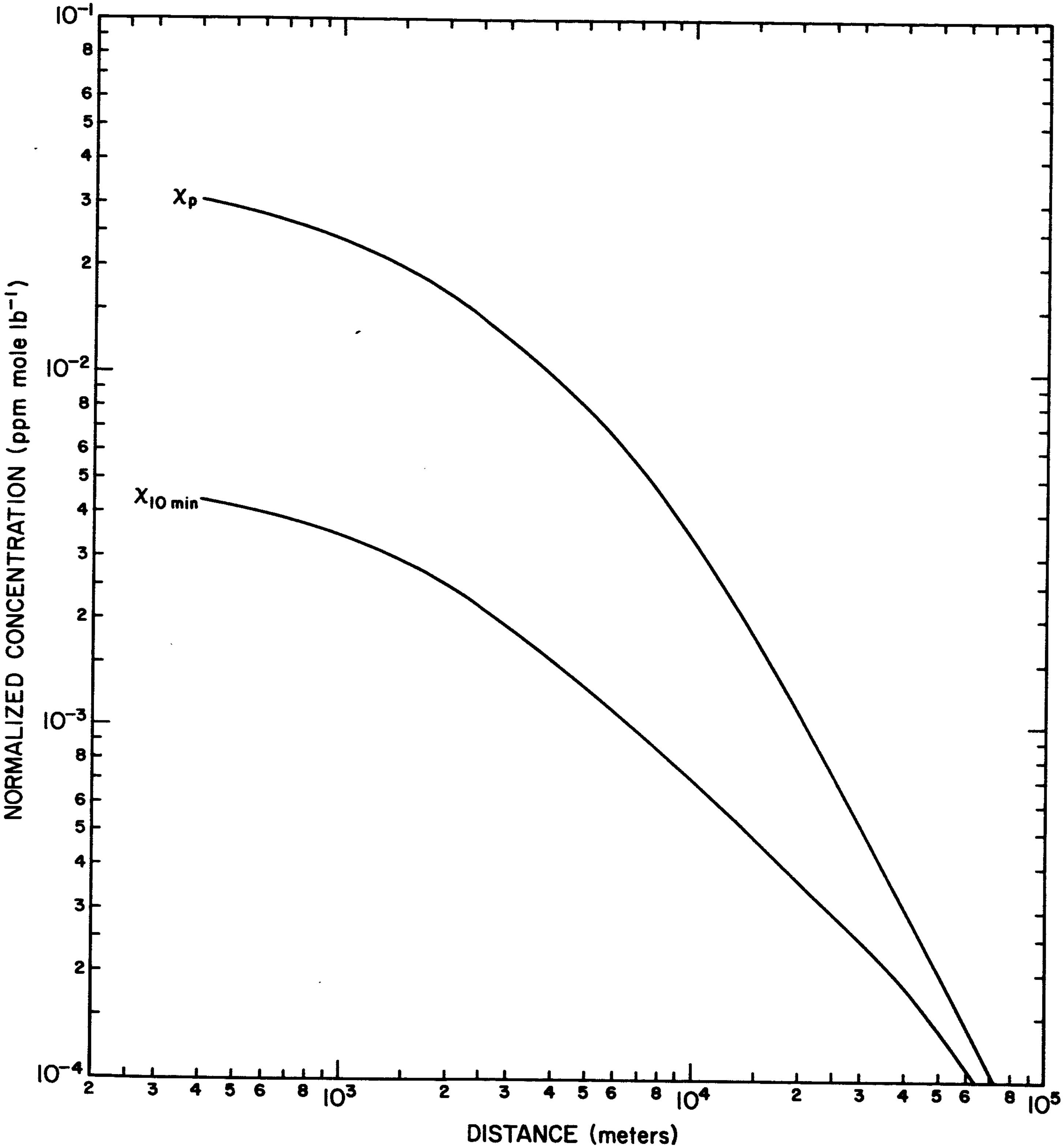

FIGURE 6-5. Normalized ground-level peak (χ_p) and ten-minute average ($\chi_{10\ min}$) concentrations downwind from a normal Saturn V launch for fall season meteorological regime. Source strength is one pound of material released in surface mixing layer.

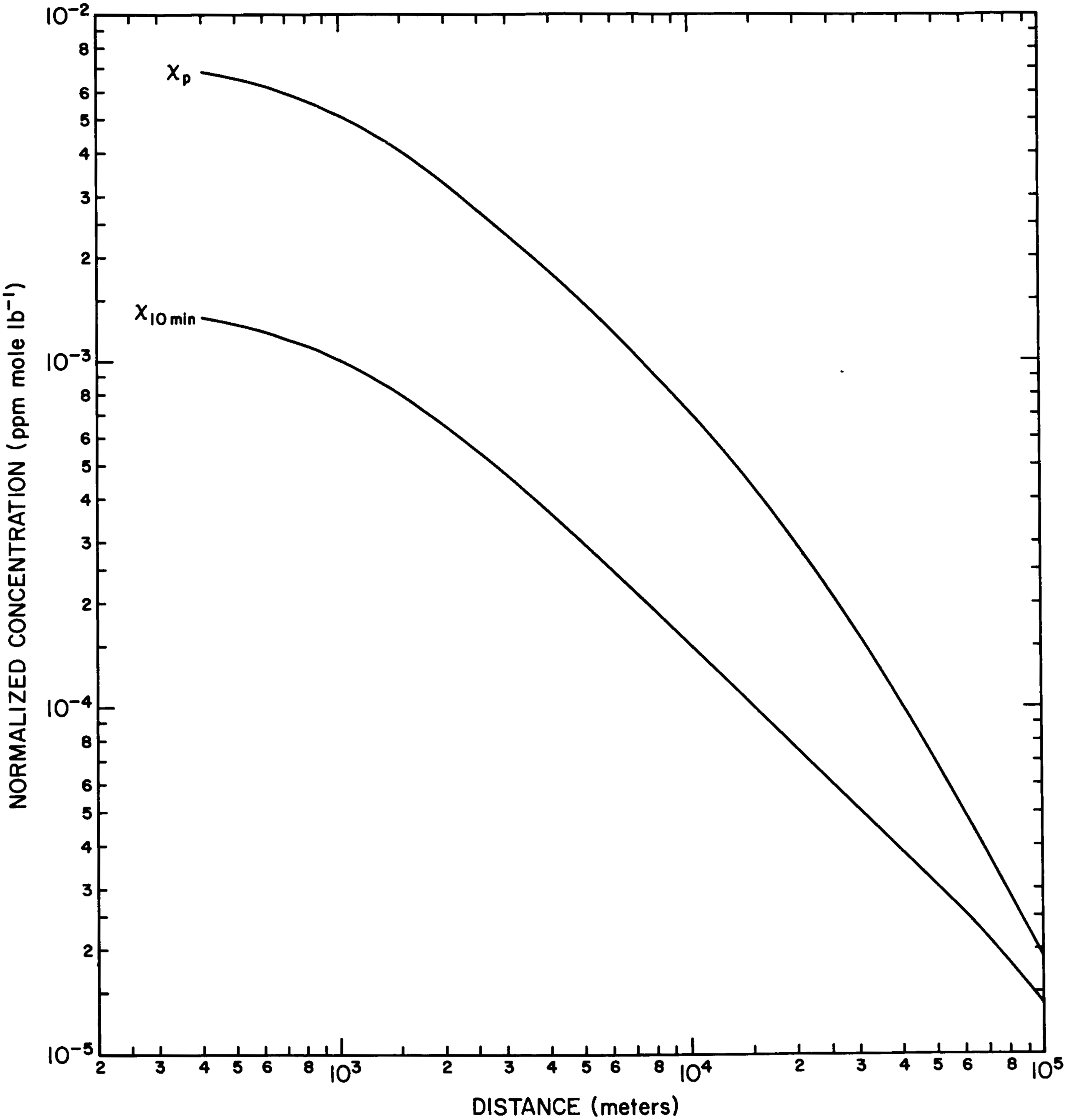

FIGURE 6-6. Normalized ground-level peak (χ_p) and ten-minute average ($\chi_{10\ min}$) concentrations downwind from a normal Saturn V launch for spring season meteorological regime. Source strength is one pound of material released in surface mixing layer.

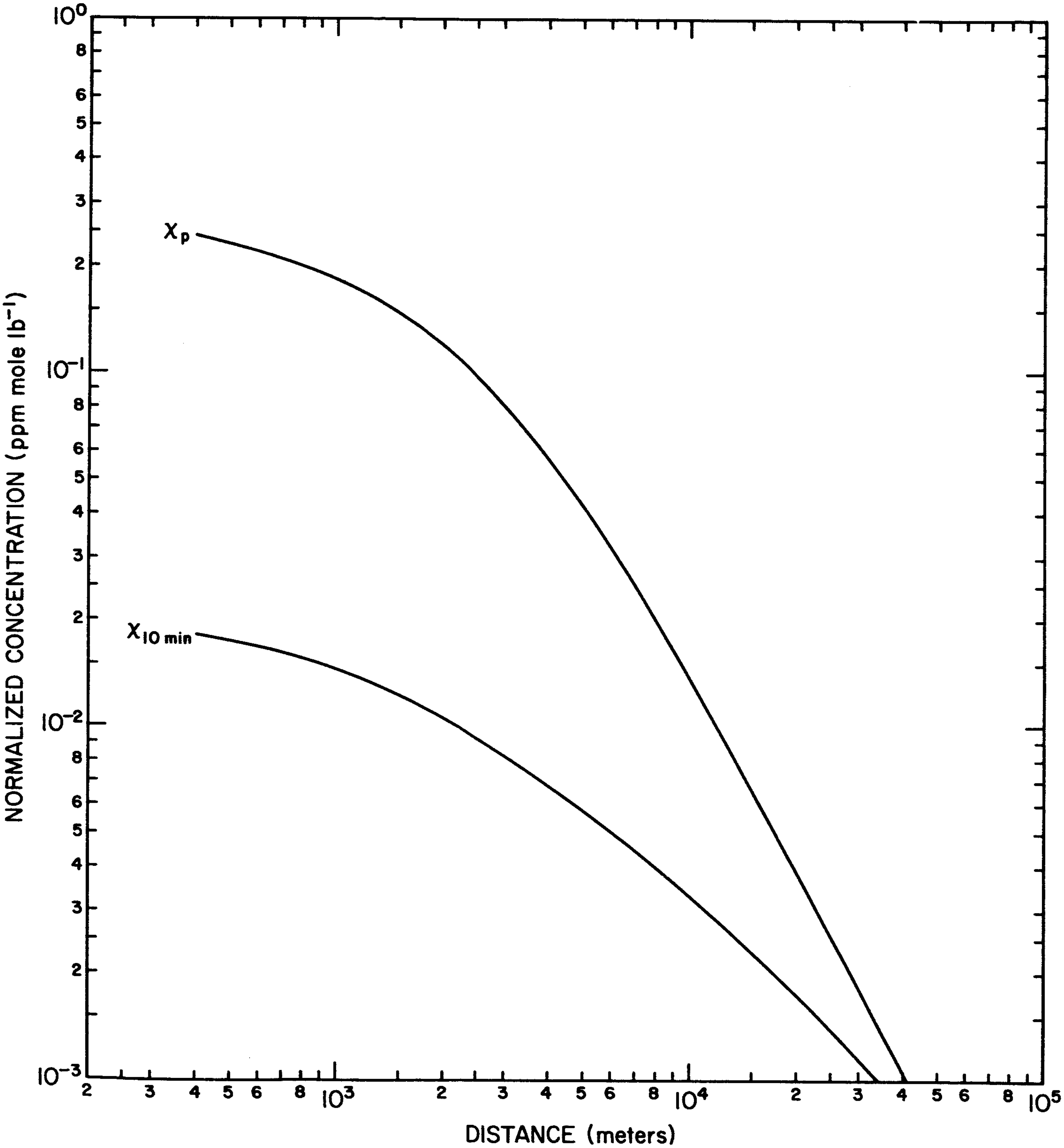

FIGURE 6-7. Normalized ground-level peak (χ_p) and ten-minute average ($\chi_{10\ min}$) concentrations downwind from a normal Saturn V launch for sea-breeze meteorological regime. Source strength is one pound of material released in surface mixing layer.

obtained by multiplying the concentration estimates in Figures 6-5, 6-6, and 6-7. by the ratio of the mixing layer depths given above to the new mixing layer depths.

The hazard distance curves in Figures 6-8 and 6-9 were obtained from Figures 6-5, 6-6, and 6-7. Figure 6-8 shows the source strength in pounds required in the surface layer to produce a ground-level peak CO concentration of 1500 parts per million (MAC_{10} from Table 1-1) at various downwind distances. For example, a source strength of 2.3×10^5 pounds of CO in the surface mixing layer produces a peak concentration of 1500 parts per million at a distance of 1 kilometer from the source in the sea-breeze meteorological regime. Figure 6-9 shows the hazard distances and surface-layer source strengths for a ten-minute average CO concentration of 1500 parts per million.

Figures 6-10 through 6-27 show the weight in pounds of each specific material listed in Table 1-1 required to produce the MAC_{10} given in the table at distances greater than 400 meters from the source.

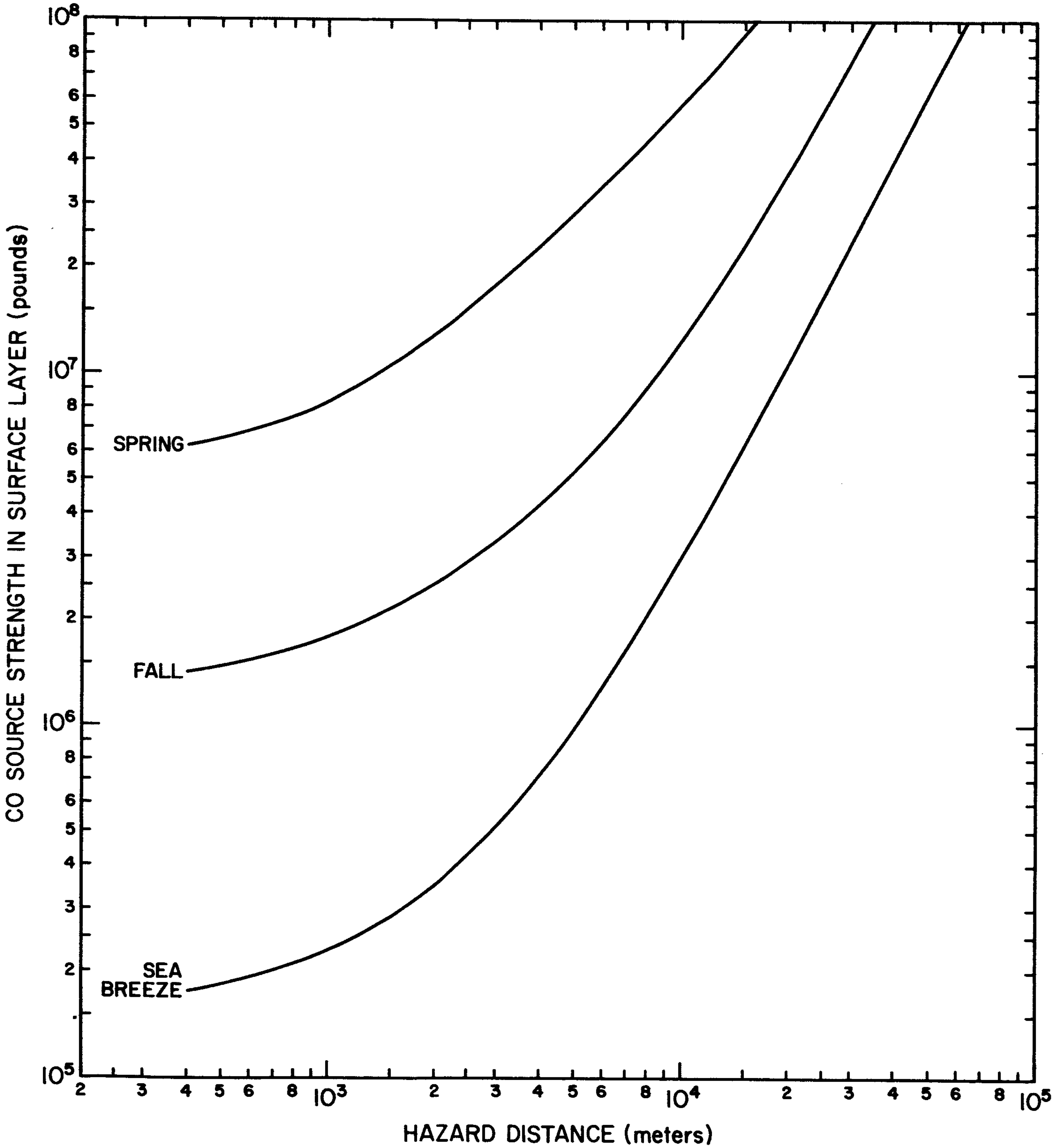

FIGURE 6-8. Hazard distances for a peak CO concentration of 1500 ppm for various surface layer source strengths.

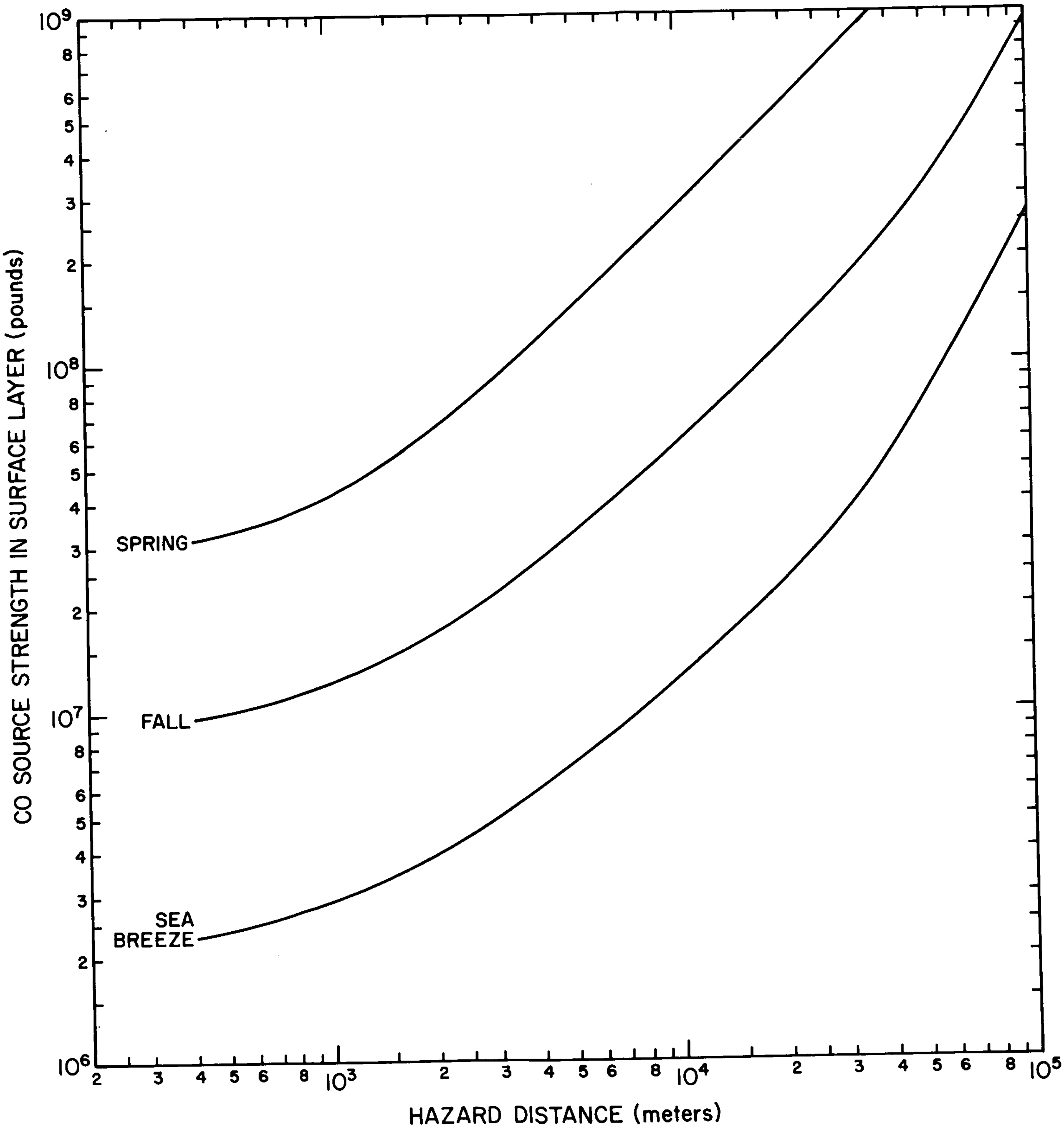

FIGURE 6-9. Hazard distances for a 10-minute average CO concentration of 1500 ppm for various surface layer source strengths.

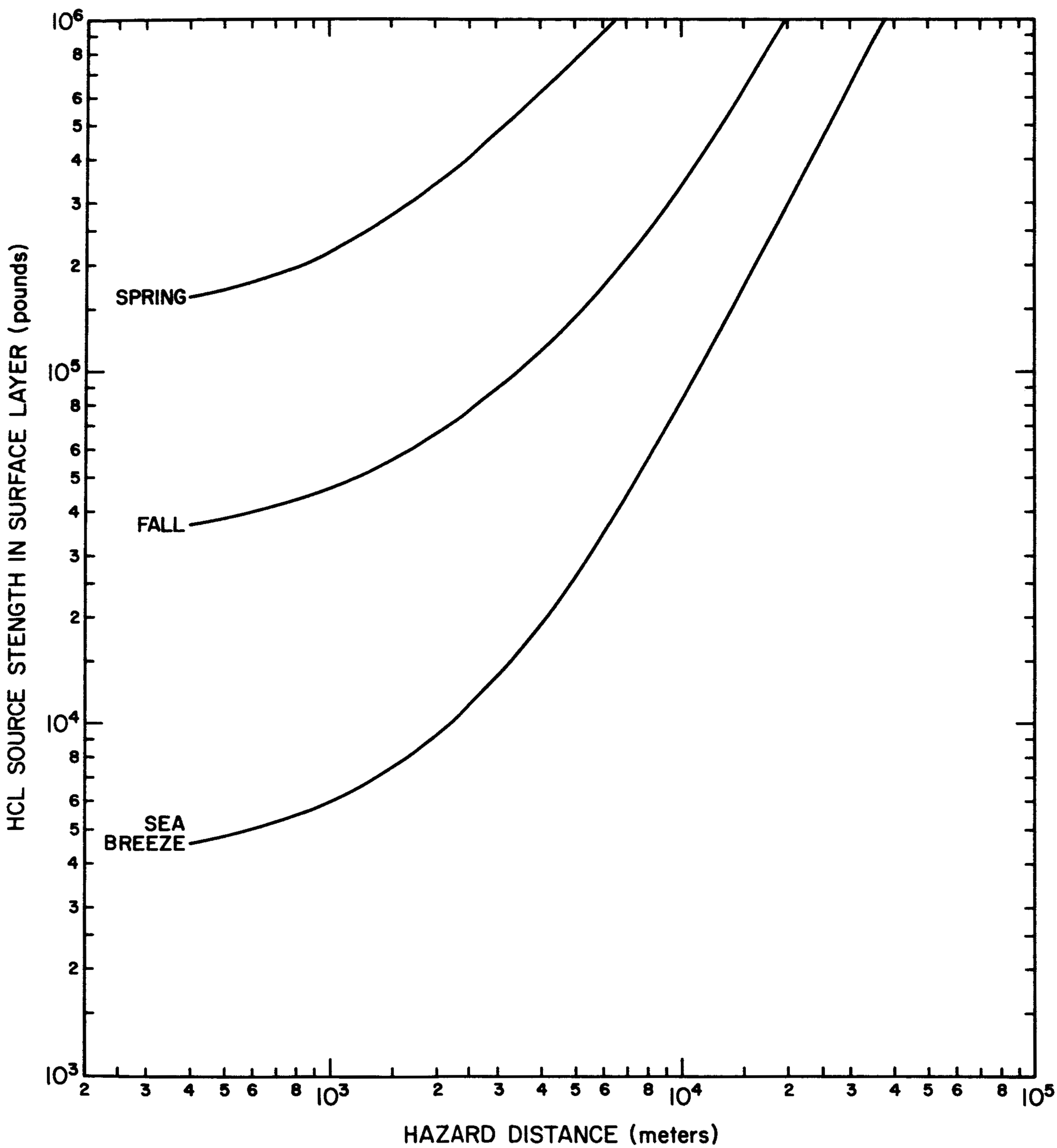

FIGURE 6-10. Hazard distances for a peak HCl concentration of 30 ppm for various surface-layer source strengths.

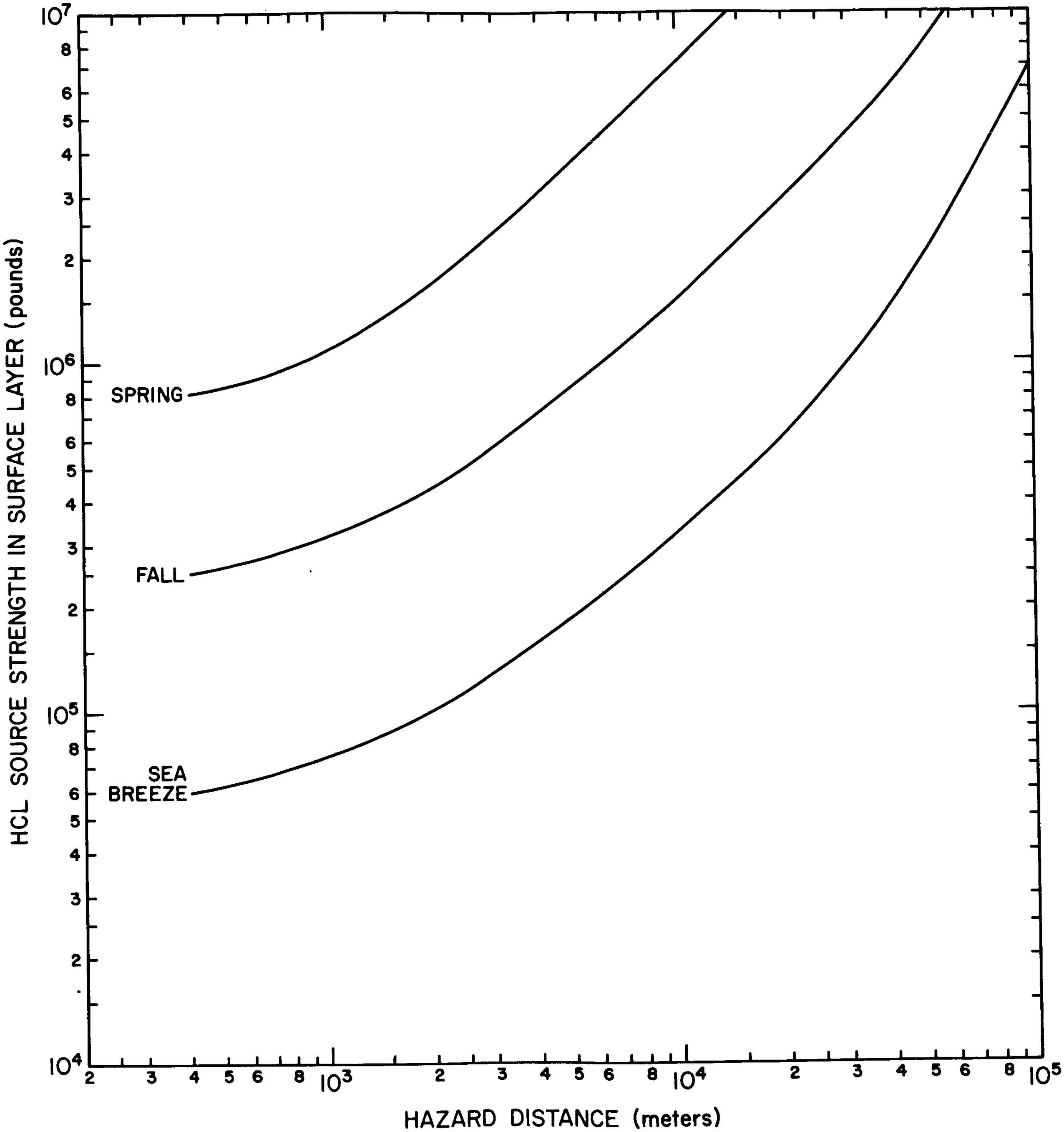

FIGURE 6-11. Hazard distances for a 10-minute average HCl concentration of 30 ppm for various surface-layer source strengths.

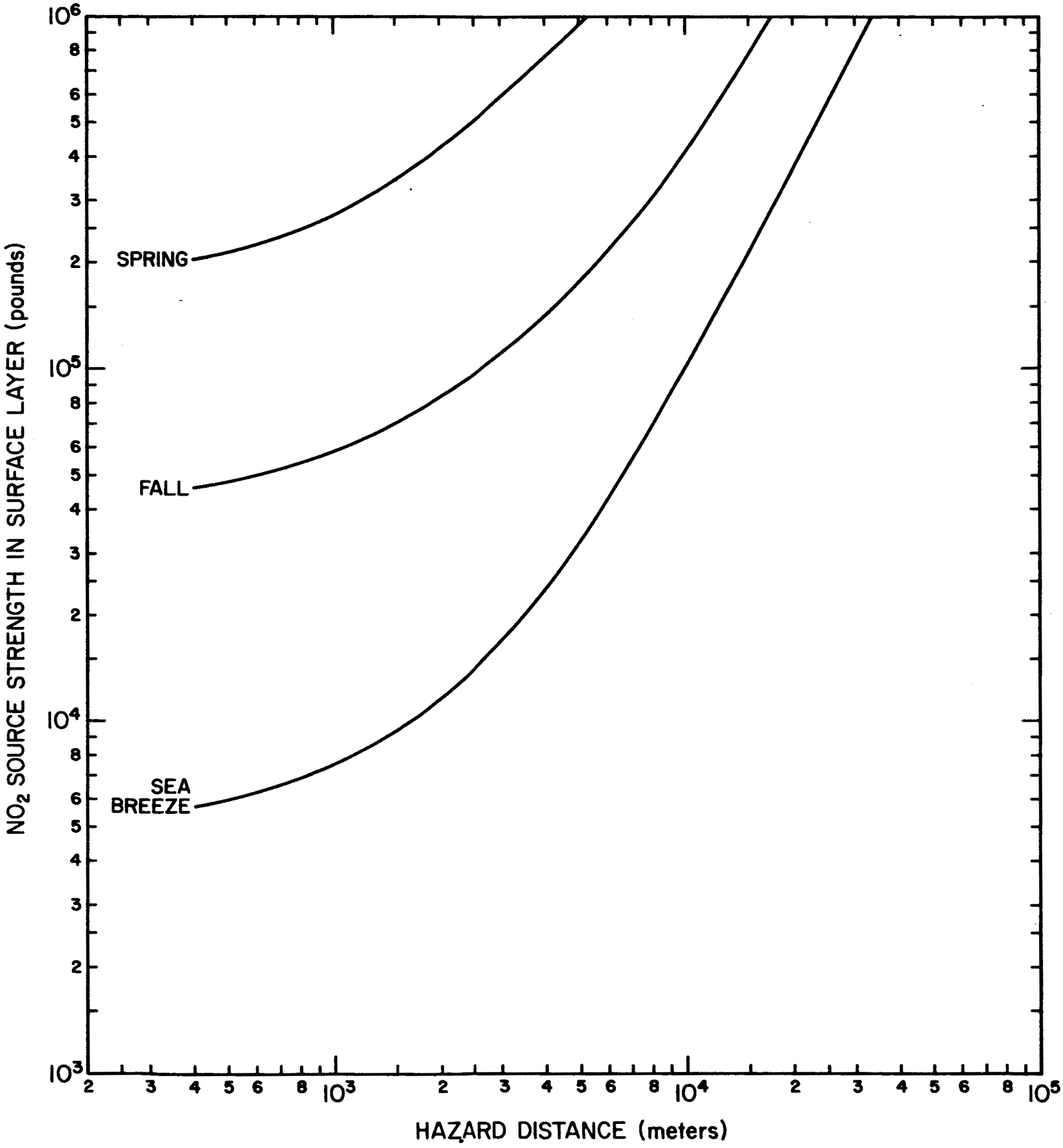

FIGURE 6-12. Hazard distances for a peak NO_2 concentration of 30 ppm for various surface-layer source strengths.

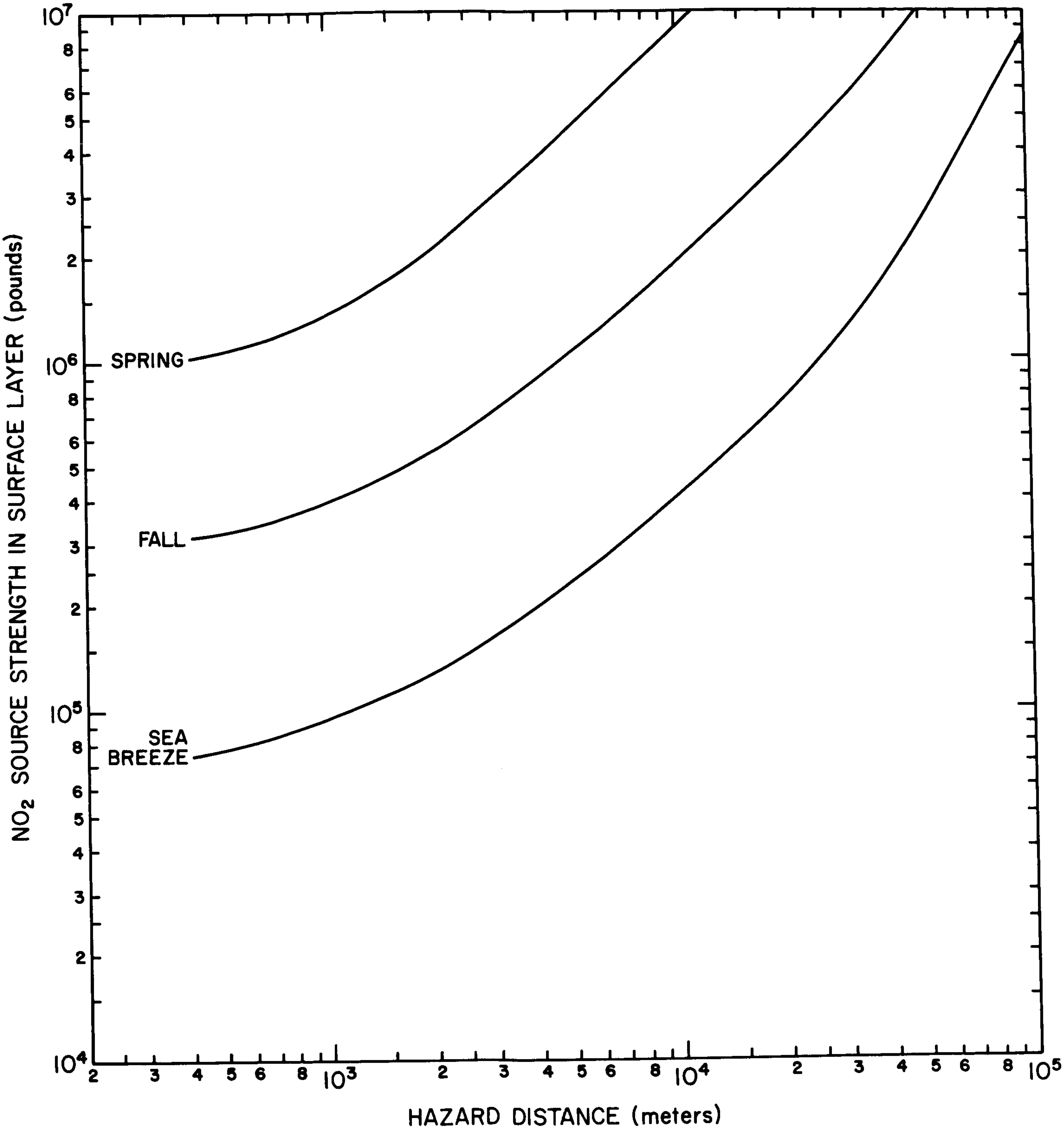

FIGURE 6-13. Hazard distances for a 10-minute average NO_2 concentration of 30 ppm for various surface-layer source strengths.

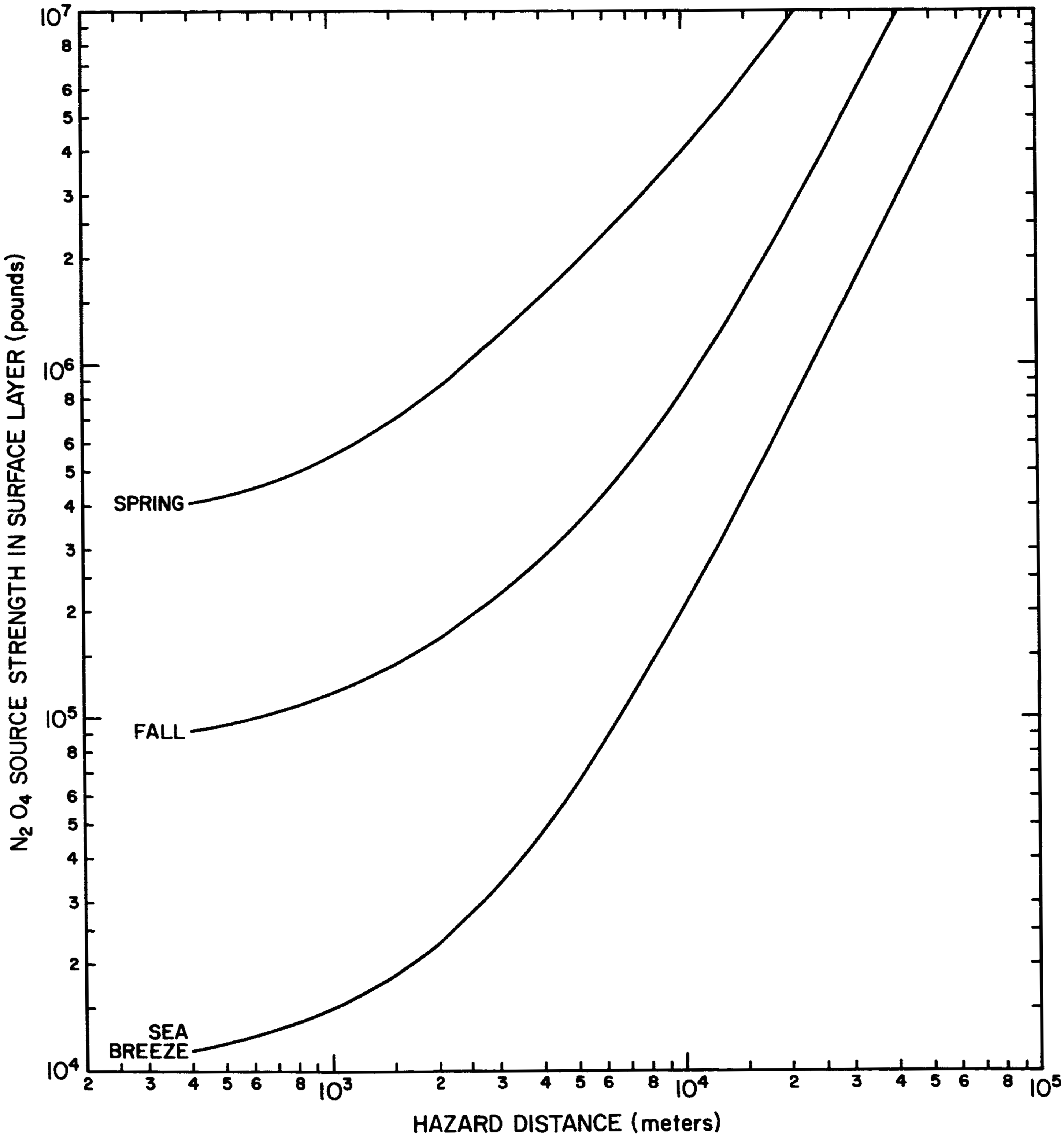

FIGURE 6-14. Hazard distances for a peak N_2O_4 concentration of 30 ppm for various surface-layer source strengths.

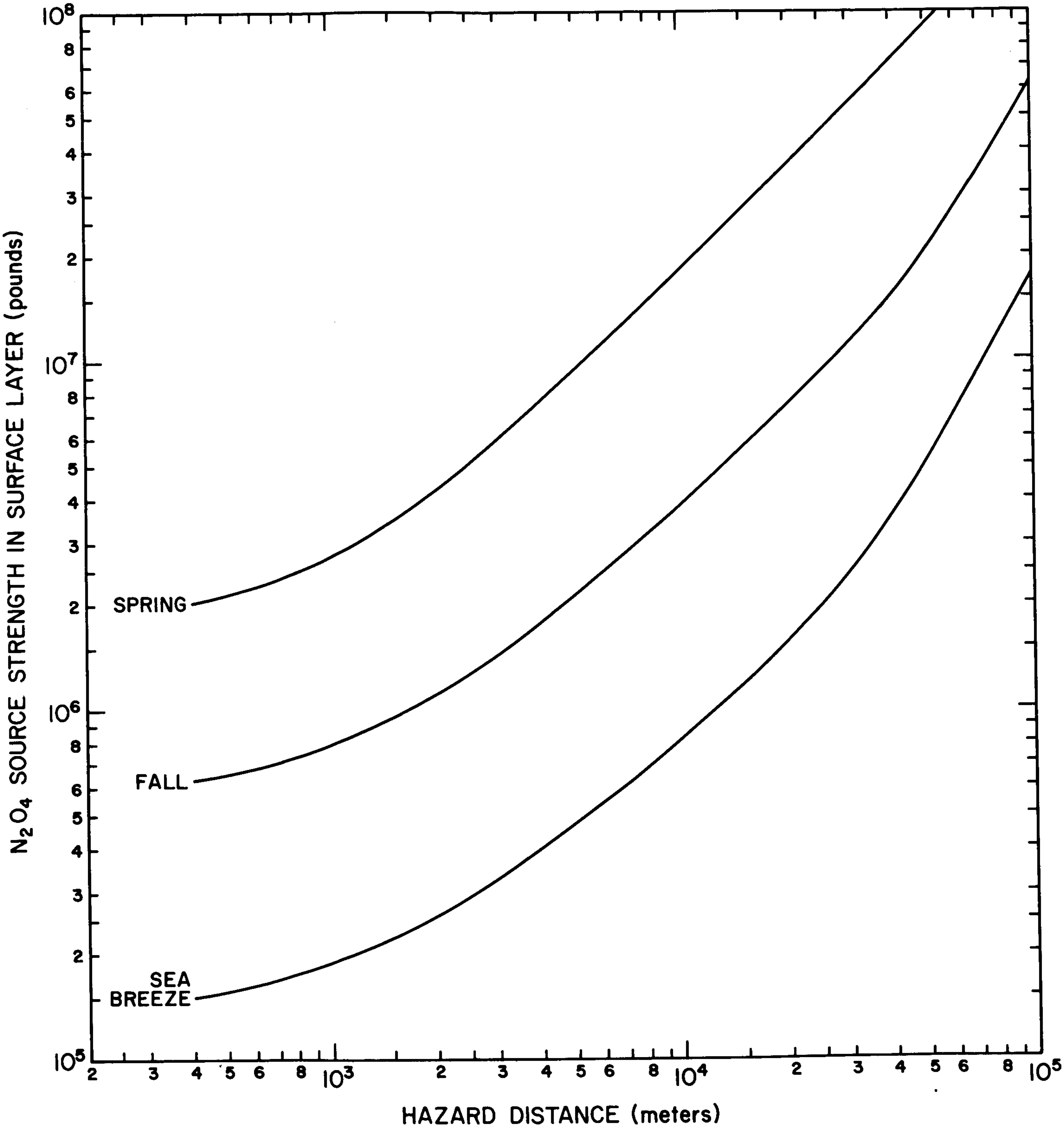

FIGURE 6-15. Hazard distances for a 10-minute average N_2O_4 concentration of 30 ppm for various surface-layer source strengths.

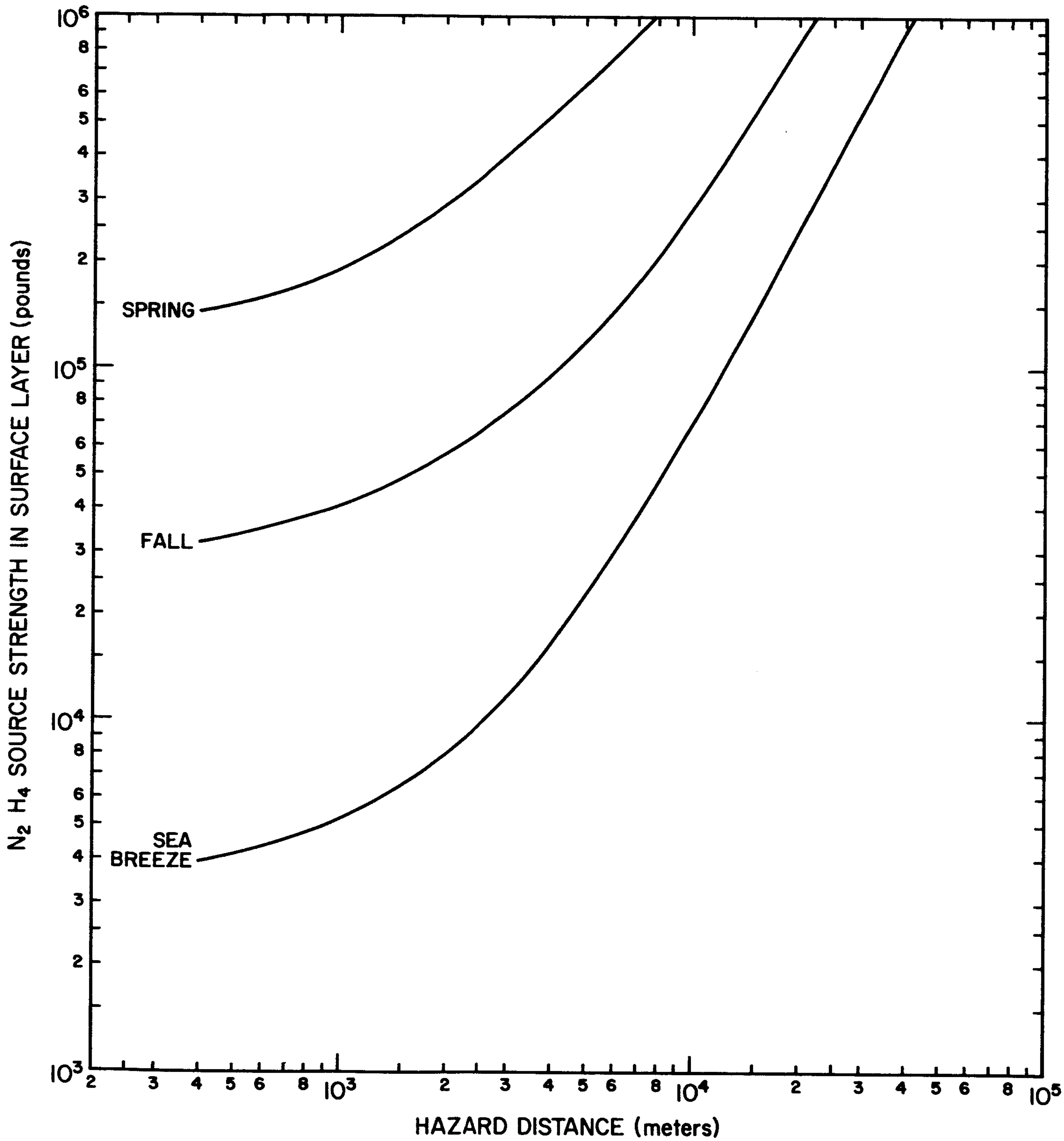

FIGURE 6-16. Hazard distances for a peak N_2H_4 concentration of 30 ppm for various surface-layer source strengths.

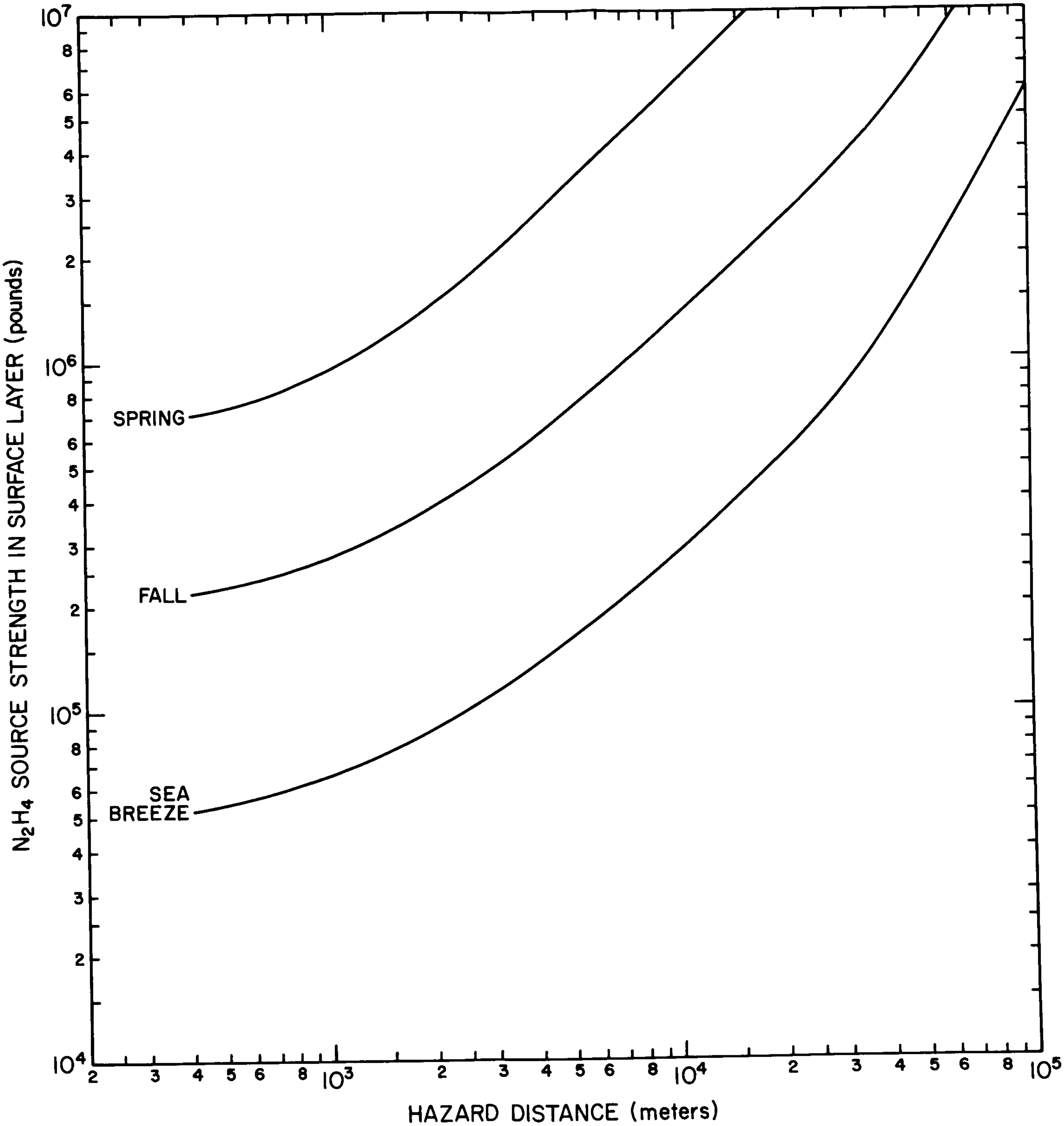

FIGURE 6-17. Hazard distances for a 10-minute average N_2H_4 concentration of 30 ppm for various surface-layer source strengths.

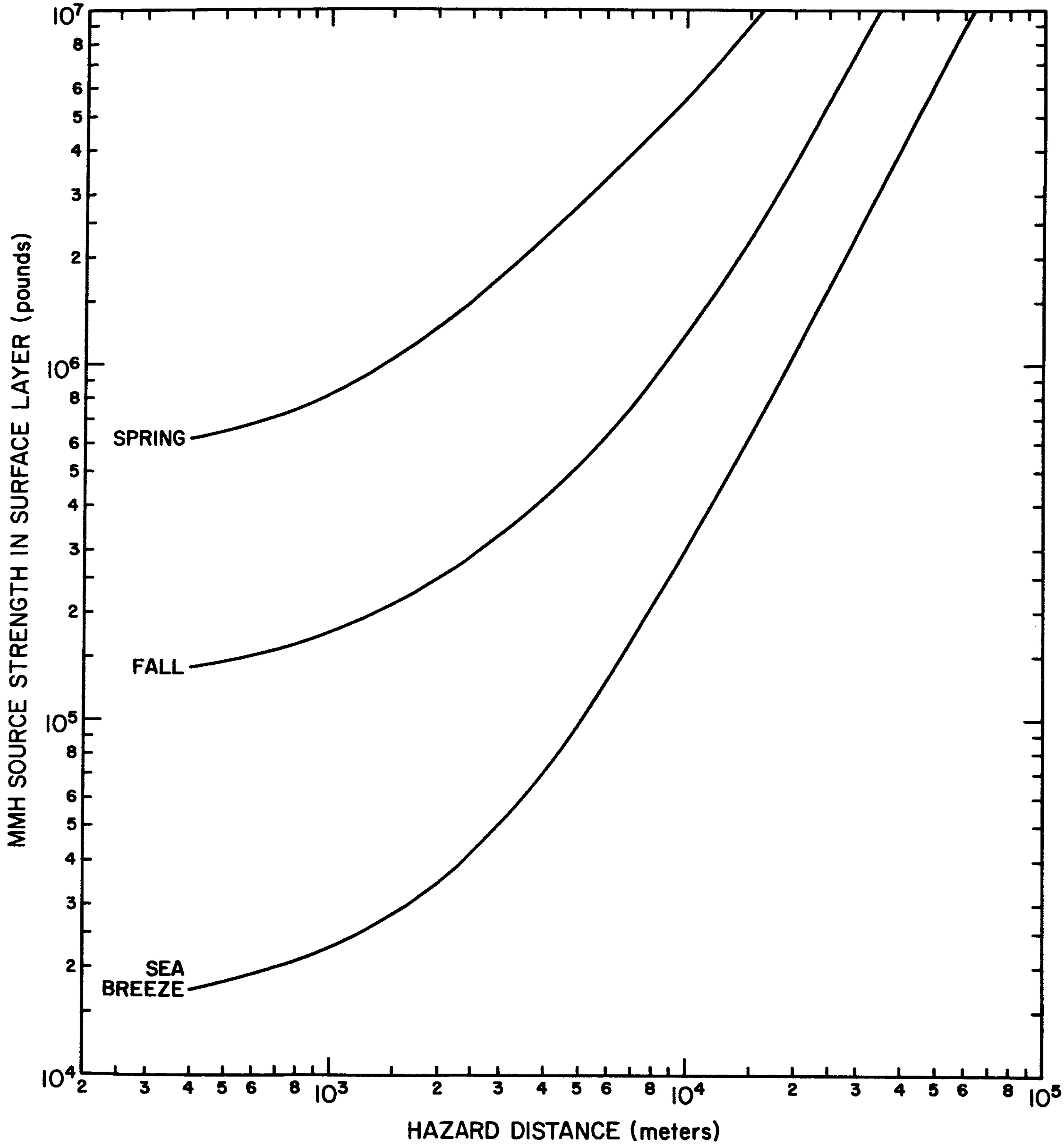

FIGURE 6-18. Hazard distances for a peak MMH concentration of 90 ppm for various surface-layer source strengths.

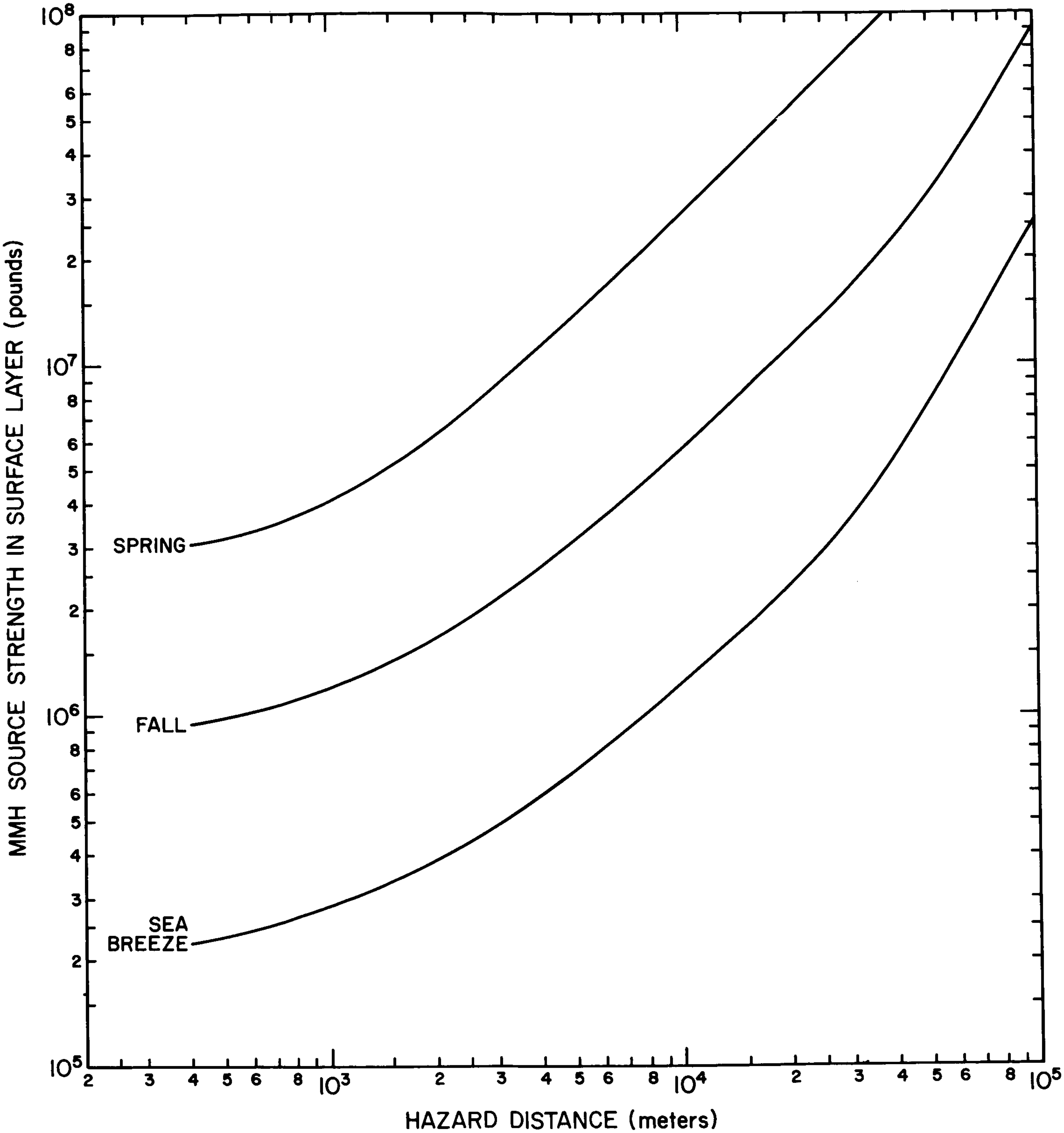

FIGURE 6-19. Hazard distances for a 10-minute **average** MMH concentration of 90 ppm for various surface-layer source strengths.

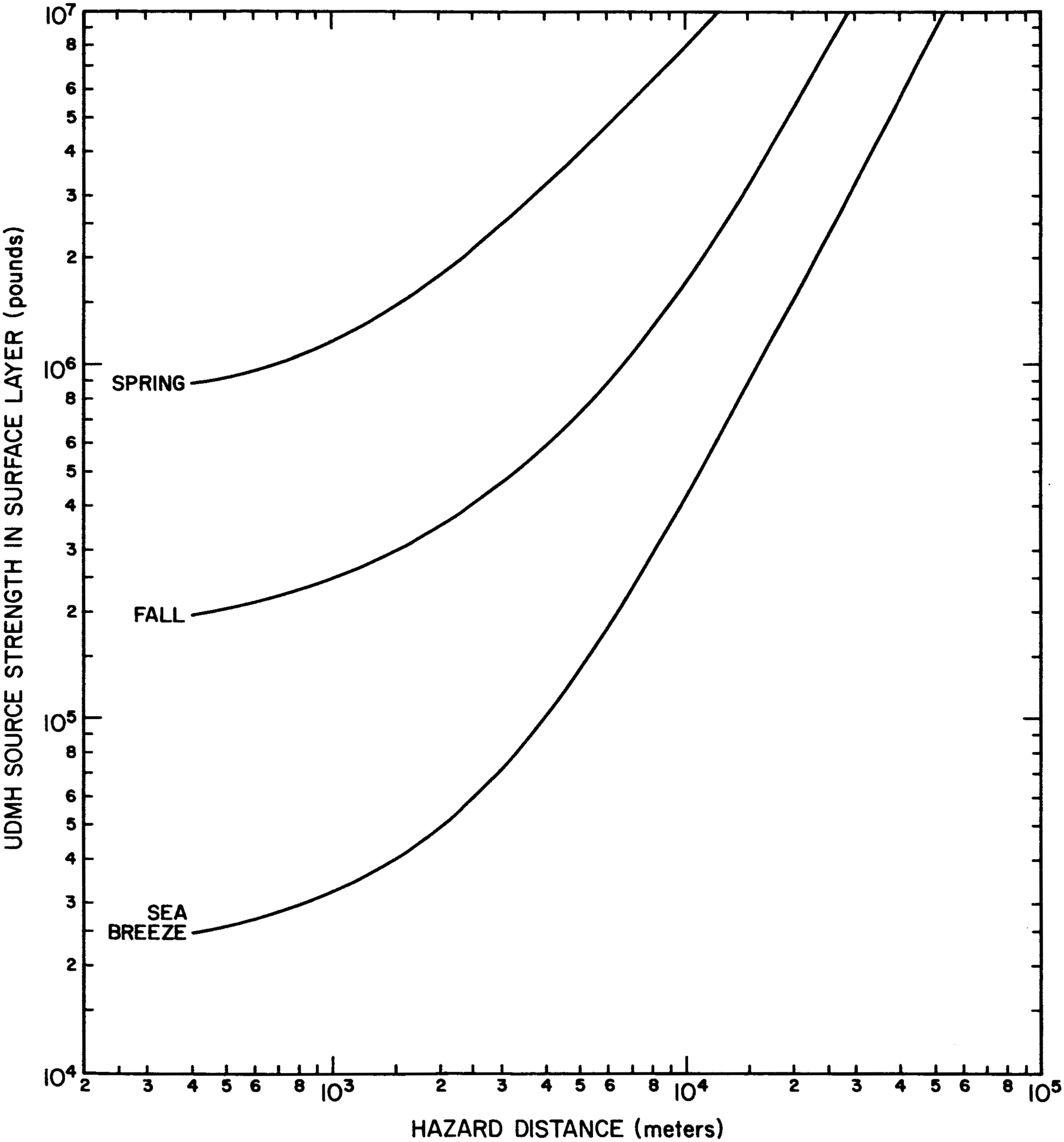

FIGURE 6-20. Hazard distances for a peak UDMH concentration of 100 ppm for various surface-layer source strengths.

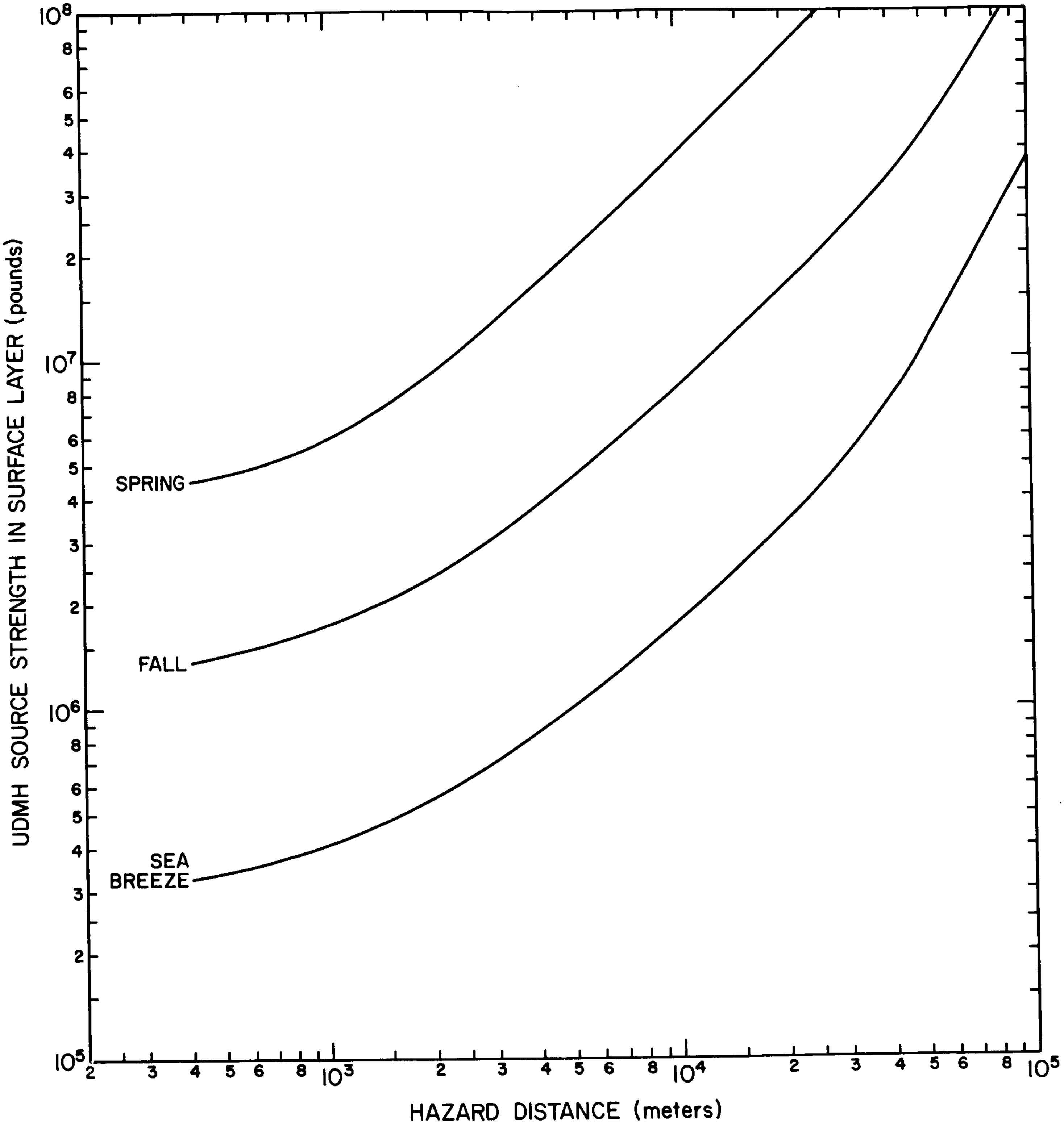

FIGURE 6-21. Hazard distances for a 10-minute average UDMH concentration of 100 ppm for various surface-layer source strengths.

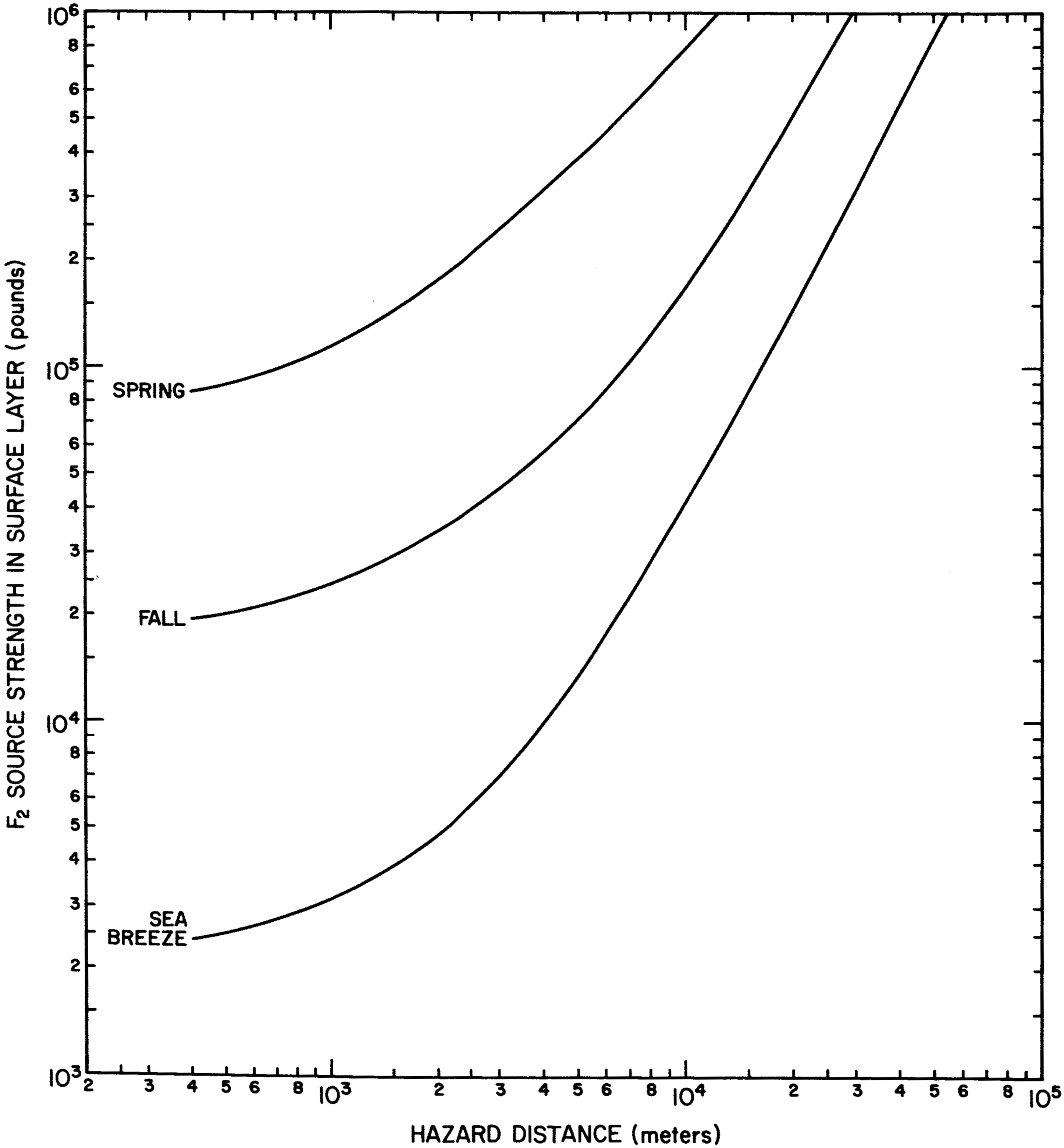

FIGURE 6-22. Hazard distances for a peak F_2 concentration of 15 ppm for various surface-layer source strengths.

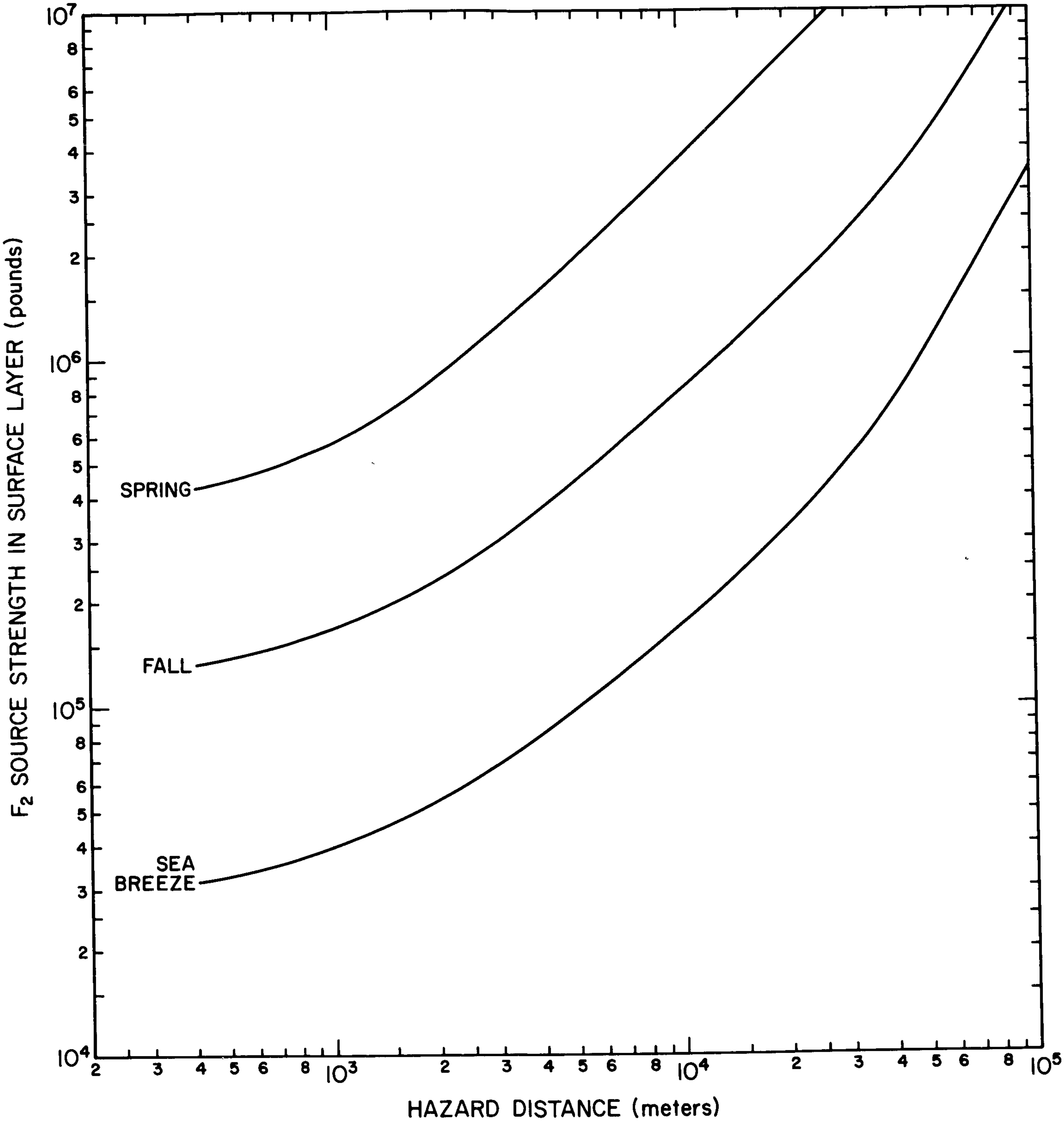

FIGURE 6-23. Hazard distances for a 10-minute average F_2 concentration of 15 ppm for various surface-layer source strengths.

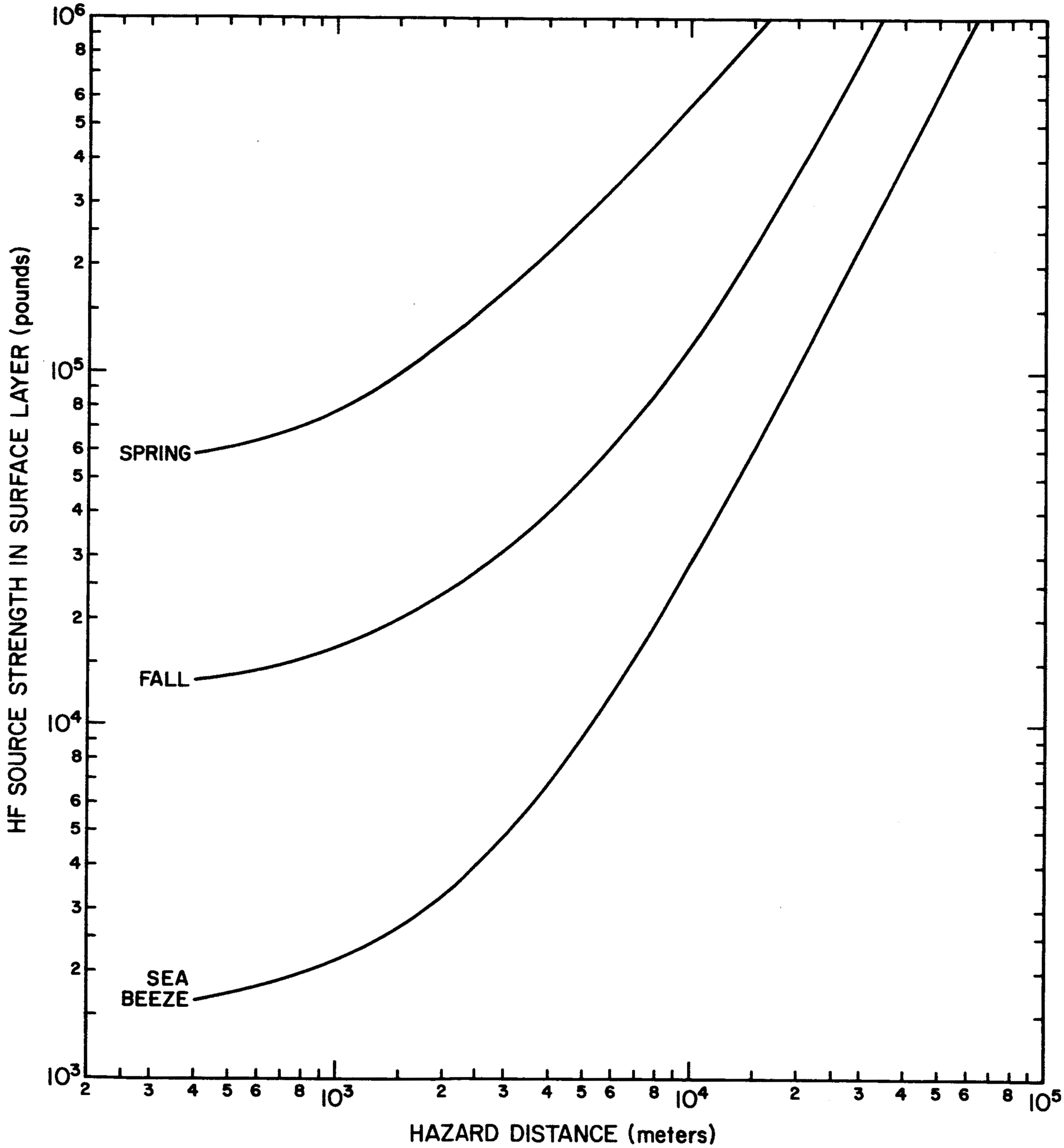

FIGURE 6-24. Hazard distances for a peak HF concentration of 20 ppm for various surface-layer source strengths.

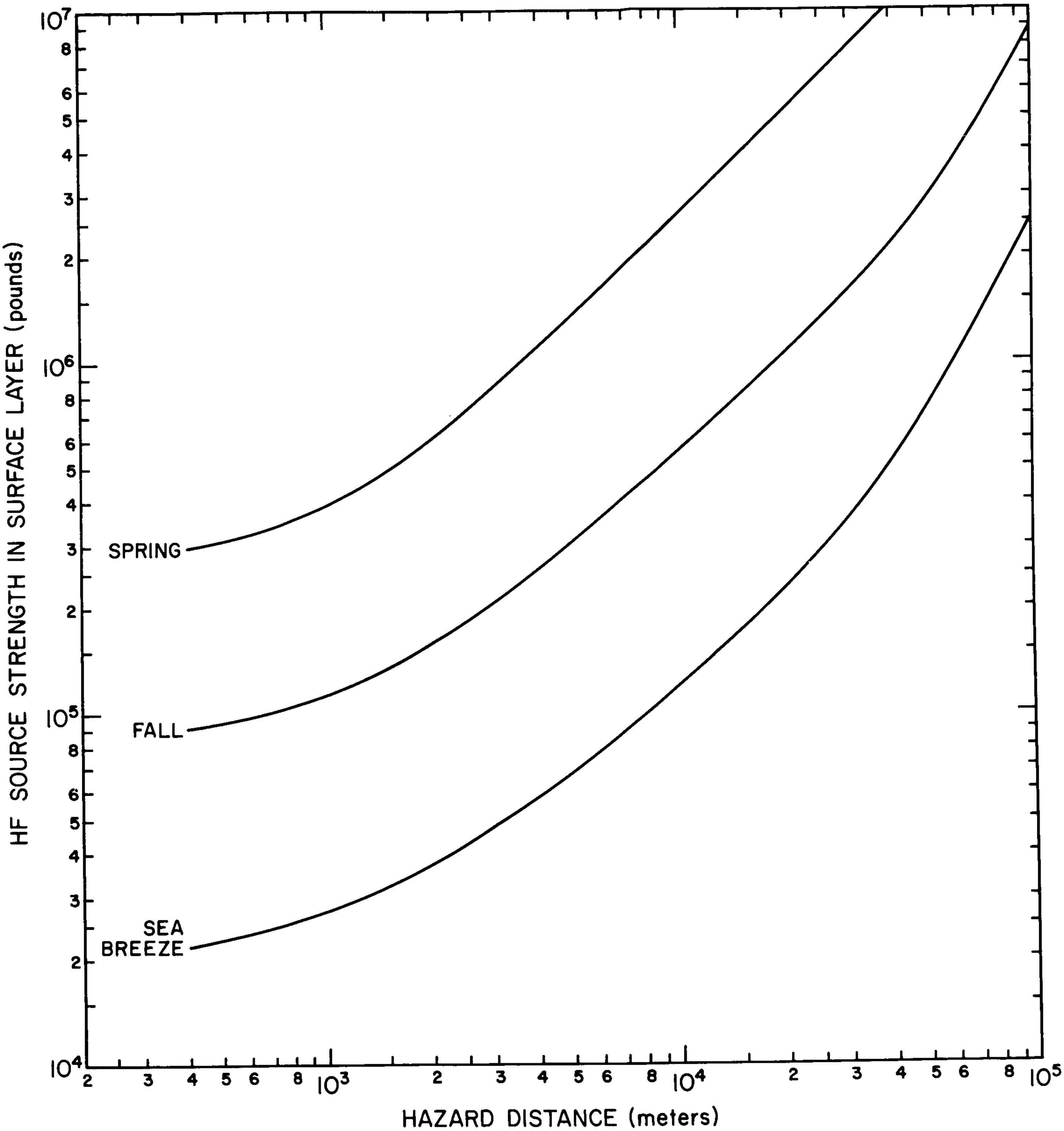

FIGURE 6-25. Hazard distances for a 10-minute average HF concentration of 20 ppm for various surface-layer source strengths.

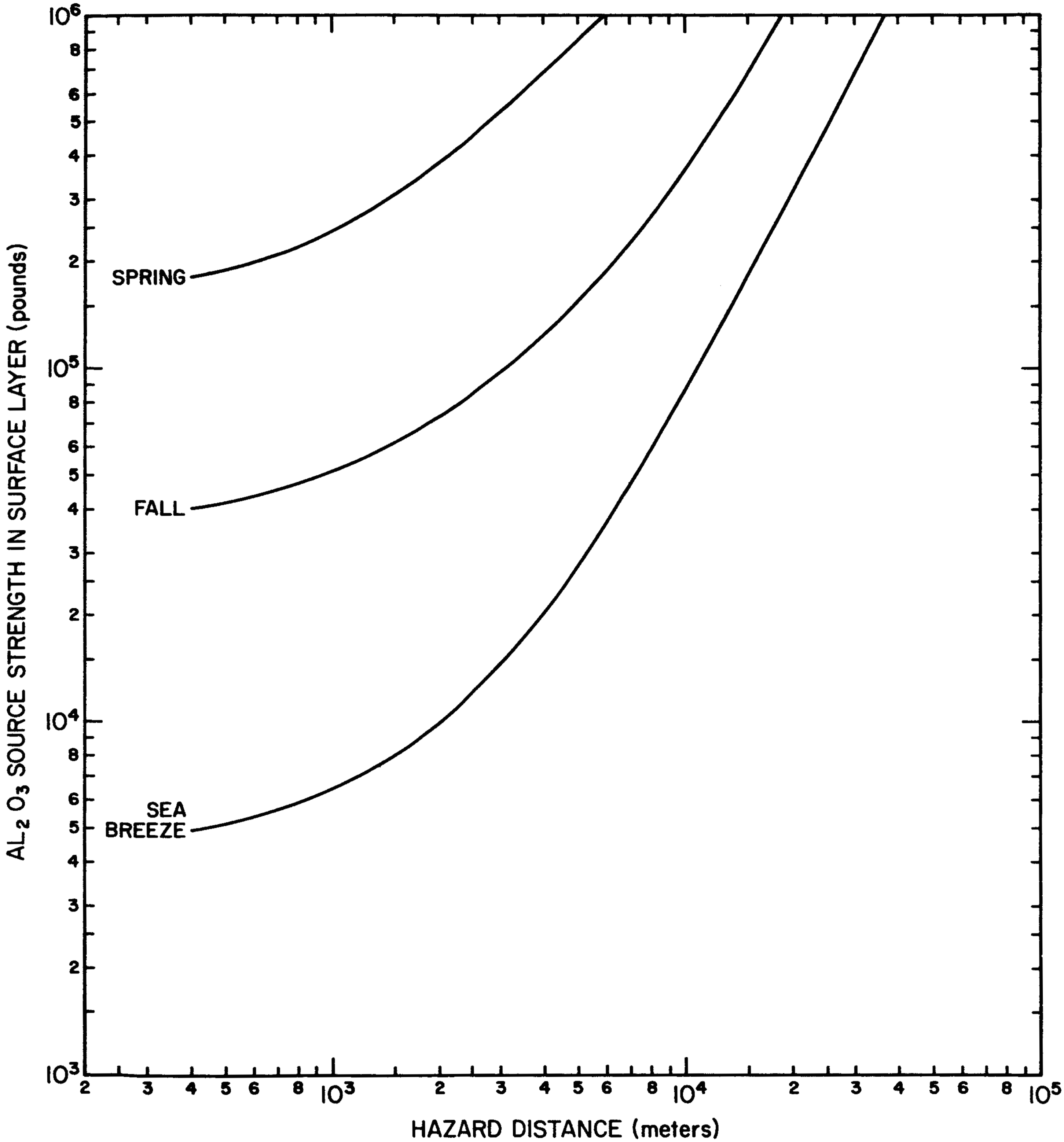

FIGURE 6-26. Hazard distances for a peak Al_2O_3 concentration of 50 mg m^{-3} for various surface-layer source strengths.

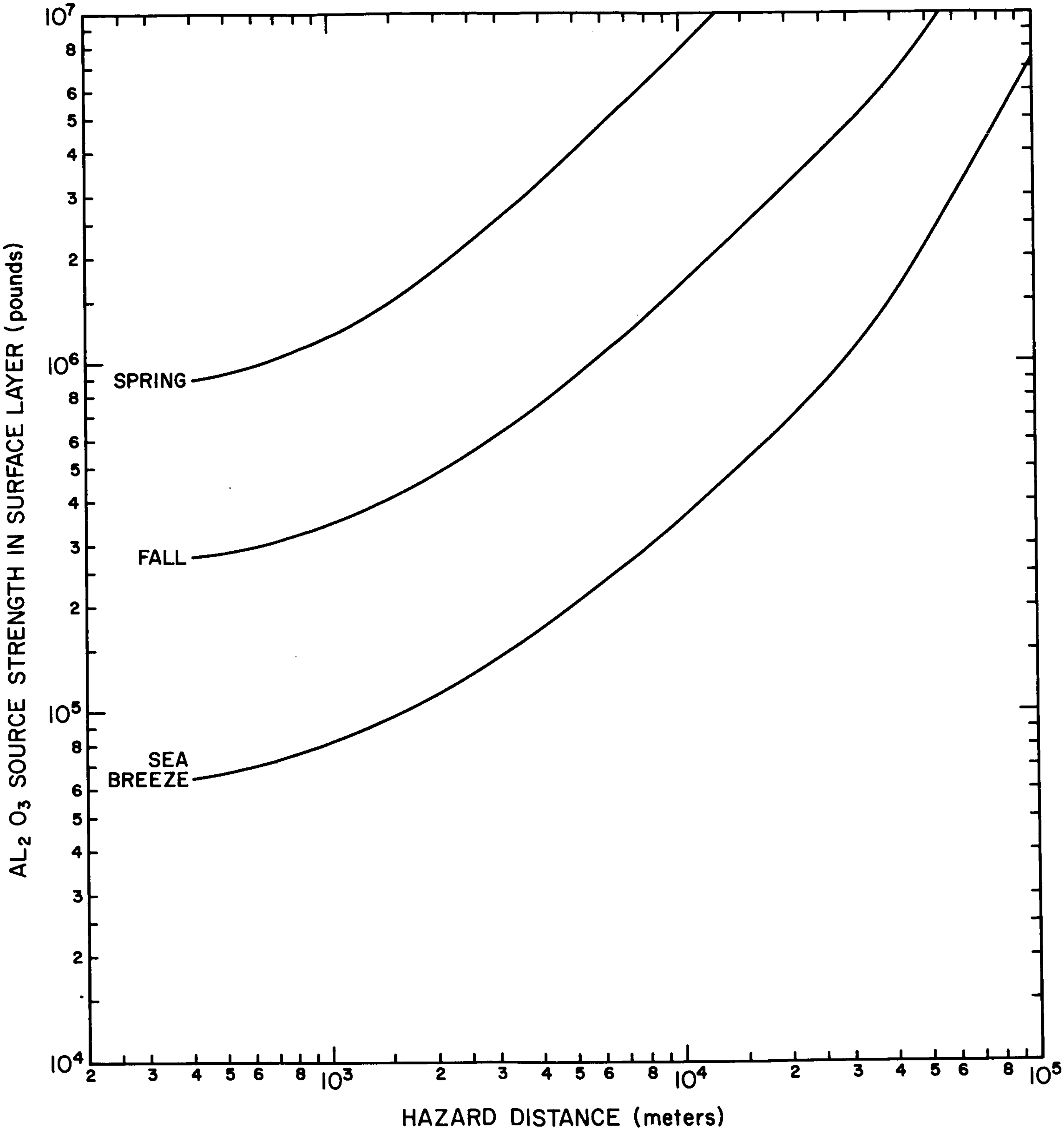

FIGURE 6-27. Hazard distances for a 10-minute average Al_2O_3 concentration of 50 mg m^{-3} for various surface-layer source strengths.

REFERENCES

Briggs, G. A., 1969: Plume Rise. TID 25075, Clearinghouse for Federal Scientific and Technical Information, Springfield, Va., 22151, 80.

Briggs, G. A. 1970: Some recent analyses of plume rise observation. Paper ME-8E presented at the Second International Clean Air Congress of the Int. Union of Air Poll. Prevention, Dec. 6-11, 1970, Washington, D. C.

Dumbauld, R. K., et al., 1970: Handbook for estimating toxic fuel hazards. Final Report under Contract No. NAS8-21453, NASA Report CR-61326, Marshall Space Flight Center, Alabama.

Dumbauld, R. K., 1971: Review of cloud rise problem. Technical Note submitted to NASA, Marshall Space Flight Center, Alabama, under Contract No. NAS8-26673.

Record, F. A., et al., 1970: Analysis of lower atmospheric data for diffusion studies. Final Report under Contract No. NAS8-30503, NASA Report CR-61327, Marshall Space Flight Center, Alabama.

Smith, J. W. and W. W. Vaughan, 1961: Monthly and annual wind distribution as a function of altitude for Patrick Air Force Base, Cape Canaveral, Florida, NASA Technical Note D-610, George C. Marshall Space Flight Center, Huntsville, Alabama.

Susko, M., J. W. Kaufman and K. Hill, 1968: Plume rise and growth of static test vehicle engine exhaust clouds. NASA TM X-53782, Aero-Astrodynamics Research Review No. 7, George C. Marshall Space Flight Center, NASA Marshall Space Flight Center, Alabama, 146-168.

Thayer, S. D., M. W. Chandler, and R. T. Chu, 1970: Rise and growth of space vehicle engine exhaust and associated diffusion models. GEOMET, Inc. Final Report to NASA under Contract NAS8-24438, NASA CR-61331, NASA-George C. Marshall Space Flight Center, Alabama, 187.

DISTRIBUTION

INTERNAL

DEP-T
S
AD-S
PM-SS
PM-MO
PM-SAT
PM-EP
PM-MT
PM-MA
S&E-CSE

S&E-ASTR
Mr. F. B. Moore

S&E-ASTN
Mr. K. Heimburg
H. G. Paul

S&E-SSL
Mr. G. Heller

S&E-R

S&E-AERO
Dr. Geissler
Mr. Horn
Mr. Dahm
H. Wilson
Mr. Baker
Mr. Lindberg
Dr. Lovingood
Mr. John Sims
Mr. W. Vaughan (2)
Mr. R. Smith
Mr. Kaufman (2)
Dr. Fichtl
Mr. Hill
Dr. DeVries
Mr. Turner
Mr. O. Smith
Mr. G. E. Daniels

EXTERNAL

Scientific and Technical Information
Facility (25)
P. O. Box 33
College Park, Maryland 20740
Attn: NASA Representative
(S-AK/RKT)

NASA
Lewis Research Center
21000 Brookpark Road
Cleveland, Ohio 44135
Attn: Director
Tech Library

NASA Headquarters
Washington, D. C. 20546
Attn: Associate Administrator, M (2)
Maj. Gen. J. W. Humphreys, MM
Col. R. A. Petrone, MA
Mr. Charak, ROO
Mr. Wm. McGowan, ROO (2)
Mr. Thomas Kerr, RNS (3)
Dr. W. Tepper, SRD
Mr. Wm. Spreen, SRM
Dir, OSSA
Dir, OART
Dir, OMSF
Safety Ofc
Marvin Redfield, OMSF
Robert Wasal, RPX
William Woodward, RP

NASA
Langley Research Center
Langley Field, Virginia 23365
Attn: Director
Tech Library

DISTRIBUTION (continued)

NASA
John F. Kennedy Space Center
Kennedy Space Center, Florida 32899
Attn: Director
Tech Library
Dr. H. Gruene, LV
Dr. Bruns, IN-DAT
Dr. Knothe, RS
Mr. P. Claybourne, DE-FSO
Mr. G. Williams, DE
Mr. R. L. Clark, TS
Mr. A. Carraway, DD-SED-4
Mr. Preston, FP
Mr. J. Spears, FP-A
Mr. L. S. Nickolson, HA
Mr. A. J. Pickett, LV-A
Mr. Ken Davis, SF-TEC
Mr. John Atkinson, SF, Dir
Mr. Ernest Amman, TS-MET

NASA
Manned Spacecraft Center
Houston, Texas 77001
Attn: Director
Mr. D. Arabian, PT
Dr. Stanley Frelen, TG
Mr. R. H. Bradley
Mr. H. E. Whitacre, KM
Mr. David Pitts, FS-2
Tech Library

NASA
Ames Research Center
Moffett Field, California 94035
Attn: Director
Tech Library
Mr. G. Goodwin, N-229-3
Mr. I. G. Poppoff, 211-6A

Jet Propulsion Laboratory
4800 Oak Grove Drive
Pasadena, California 91103
Attn: Director
Tech Library

NASA
Goddard Space Flight Center
Greenbelt, Maryland 20771
Attn: Director
Tech Library
Dr. Wm. Nordberg
Dr. A. Aiken
Mr. W. Bandeen

NASA
Wallops Station
Wallops Island, Virginia 23337
Attn: Tech Library
Mr. M. McGoogan, RED
Mr. J. F. Spurling

NASA
Flight Research Center
Edwards, California 93523
Attn: Director
Tech Library

National Weather Service-NOAA
Space Operation Support Division
Rockville, Maryland 20852
Attn: Dr. Kenneth Nagler
Dr. I. Vander Hoven

Alan Sanderson
National Weather Service
Space Operation Support Division
MOW Bldg. 30
NASA Manned Spacecraft Center
Houston, Texas 77058

University of Alabama
Research Institute
Box 1247
Huntsville, Alabama 35805

U. S. Army Missile Command
Redstone Arsenal, Alabama 35810
Attn: Dr. O. Essenwanger, AMSMI-RRA
Mr. J. Connaughton

McDonnell Douglas Astronautics
Company
5301 Bolsa Avenue
Huntington Beach, California 92647
Attn: Mr. John B. Peterson, AS-253

North American Rockwell Corporation
12214 Lakewild Boulevard
Downey, California 90241
Attn: Mr. C. D. Martin

TRW Systems
One Space Park
Redondo Beach, California 90278
Attn: Mr. Marvin E. White

General Dynamics/Convair Division
P. O. Box 1128
San Diego, California 92112
Attn: Tech Library

Lockheed Missiles & Space Company
3251 Hanover Street
Palo Alto, California 94304
Attn: Dr. R. G. Johnson

Lockheed-California Company
P. O. Box 551
Burbank, California 91503
Attn: Library

General Dynamics
5873 Kearny Villa Road
San Diego, California 92123

Aerospace Corporation
P. O. Box 95085
Los Angeles, California 90045

Lockheed Missiles & Space Company
P. O. Box 504
Sunnyvalé, California 94088
Attn: Mr. Larry Fried,
Dept 62-63, Bldg 104

Stanford Research Institute
Menlo Park, California 94025
Attn: Mr. R. T. H. Collis, Dir
Aerophysics Laboratory

McDonnell Douglas Corporation
S&ID
Downey, California

NOAA Research Laboratories
Boulder, Colorado 80302
Attn: Dr. Robert Cohen
Technical Library

Colorado State University
Department of Atmospheric
Science
Fort Collins, Colorado 80521
Dr. E. R. Reiter

U. S. Atomic Energy Commission
Washington, D. C. 20545
Attn: Mr. W. L. Kitterman, F-309

Meteorological & Geoastrophysical
Abstracts
P. O. Box 176
Washington, D. C. 20013

Office of Staff Meteorologist
Air Force Eastern Test Range
Patrick AFB, Florida 32925

6WWD11
Eastern Test Range
Patrick AFB, Florida 32925
Attn: Mr. I. Kuehnast

PAWA/GMRD, AFMTC
MU-235, Tech Library
Patrick AFB, Florida 32925
Attn: Mr. Orville Daniel

DISTRIBUTION (continued)

Florida State University
Department of Meteorology
Tallahassee, Florida 32306

Commander
Headquarters, Air Weather Service
Scott AFB, Illinois 62225
Attn: Aerospace Science Dir
Tech Library (2)

Air Force Cambridge Research Laboratory
L. G. Hanscom Field
Bedford, Massachusetts 01730
Attn: Mr. N. Sissenwine (4)
Tech Library (3)
Dr. M. Bavad

GCA Corporation
Route 62, Burlington Road
Bedford, Massachusetts 01730
Attn: Dr. George Ohring
Dr. Harrison Cramer (10)
Mr. R. K. Dumbauld
Mr. J. R. Bjorklund

Atmospheric Science Laboratory
U. S. Army Electronics Command
White Sands Missile Range,
New Mexico 88002
Attn: Mr. W. Webb

New Mexico Institute of Mining
and Technology
Soccorro, New Mexico 87801
Attn: Dr. Marx Brook
Mr. C. B. Moore

National Weather Records Center
NOAA
Asheville, North Carolina 28801

Grumman Aircraft Corporation
Bethpage, L. I., New York 11714
Attn: Tech Library

The Pennsylvania State University
503 Deike Building
University Park, Pennsylvania 16802

National Weather Service-AEC
Oak Ridge, Tennessee 37830
Attn: Dr. Frank Gifford

Texas A&M University
Department of Meteorology
College Station, Texas 77843
Attn: Dr. J. R. Scoggins

The Boeing Company
P. O. Box 3707
Seattle, Washington 98124
Attn: Library